

Title	Neutral-Current Effects in Bethe-Heitler Process with Circularly Polarized Photons
Author(s)	Konashi, Hiroshi
Citation	大阪大学, 1980, 博士論文
Version Type	VoR
URL	https://hdl.handle.net/11094/24448
rights	
Note	

Osaka University Knowledge Archive : OUKA

<https://ir.library.osaka-u.ac.jp/>

Osaka University

Neutral-Current Effects in Bethe-Heitler Process with
Circularly Polarized Photons

Hiroshi KONASHI

(Doctor Thesis)

Department of Physics

Osaka University

Toyonaka, Osaka, Japan

Contents

- §1. Introduction
- §2. The cross section for lepton pair production with circularly polarized photon beams
 - 2-1. The leptonic tensors
 - 2-2. The hadronic tensors
 - 2-3. The differential cross sections
- §3. The gauge model
- §4. The inclusive photoproduction of lepton pairs
 - 4-1. The definition of the parity-violating asymmetry of the cross sections for the inclusive photoproduction of lepton pairs
 - 4-2. Structure functions
 - 4-3. Numerical results
- §5. The exclusive photoproduction of lepton pairs
 - 5-1. The definition of the parity-violating asymmetry of the lepton angular distribution for the exclusive reaction
 - 5-2. Form factors
 - 5-3. Numerical results
- §6. Conclusions
- Appendix A.
- Appendix B.

Abstract

The weak neutral-current effects in the lepton pair production with circularly polarized photon beams on unpolarized targets are investigated in unified gauge theories. We derive the differential cross sections for leptons produced by right- and left-handed photons on unpolarized targets. We define the parity-violating asymmetry as the ratio of the difference of these cross sections to the sum of them. Numerical calculations are given in the standard Weinberg-Salam model in the case of the isoscalar and proton targets. The asymmetry is shown as a function of the lepton energy in some kinematical configurations. The weak neutral-current effects are of the order of 10^{-4} for the inclusive lepton pair production and of the order of 10^{-5} for the exclusive one at the incident photon energy of 20 Gev.

§ 1. Introduction

In 1973 - 74 weak neutral-currents were discovered experimentally in inclusive neutrino reactions¹⁾ and in single pion production processes by neutrinos.²⁾ A number of experimental data on weak neutral-currents have been accumulated till now, so that we can understand main features of the weak neutral-current interactions.³⁾

Our most detailed experimental informations on weak neutral-current interactions come from data on νN and $\bar{\nu} N$ reactions, including inclusive reactions $\bar{\nu} N \rightarrow \bar{\nu} X$; semi-inclusive reactions $\bar{\nu} N \rightarrow \bar{\nu} \pi X$; exclusive pion production $\bar{\nu} N \rightarrow \bar{\nu} \pi N$ and elastic scatterings $\bar{\nu} p \rightarrow \bar{\nu} p$. It has been clear now that the experimental data for these reactions are in good agreement with the predictions of the Weinberg-Salam model⁴⁾ with the Glashow-Iliopoulos-Maiani mechanism.⁵⁾

The data on neutrino-electron elastic scatterings are less precise than those on neutrino-nucleon reactions because at the same incident energy of the neutrino beam, the cross sections of the former scatterings are smaller than those of the latter reactions. Within the experimental uncertainties, data on $\bar{\nu}_e e$, $\bar{\nu}_\mu e$ and $\nu_\mu e$ elastic scatterings have been in agreement with the predictions of the Weinberg-Salam model. We show in the Table I the experimental results on the neutrino induced neutral-current processes tabulated by C. Baltay.³⁾

The electron-nucleon weak neutral-currents have been difficult to study experimentally, because electrons interact with nucleons electromagnetically, so that one must look for effects that are characteristic of the weak interactions, and for a parity violation.

This parity violation has studied at first in atomic physics.⁶⁾ The experiments on bismuth 209 at Oxford and Seattle set upper limits on the optical rotation that were well below the predictions of the Weinberg-Salam model.

The experiment, however, on bismuth 209 at Novosibirsk are in disagreement with the limit set at Oxford for the same frequency but in agreement with the prediction of the Weinberg-Salam model. In view of the conflict between the experiments, one should not be too concerned about any possible discrepancies with the Weinberg-Salam model. In 1978 - 79, parity violation in deep inelastic scattering of longitudinally polarized electrons from unpolarized deuterons has been observed at SLAC⁷⁾ and the results are consistent with the prediction of the Weinberg-Salam model.

It is now of particular importance to determine the relevant form of the electron-quark neutral-current couplings and will be the highlight to determine the form of the muon-quark and tau-quark neutral-current couplings.

In this thesis, we study a possible phenomenon due to the weak neutral-currents related to the electron and the muon. We discuss the parity-violating asymmetry of the differential cross sections for the lepton pair production with circularly polarized photons on unpolarized targets: $\gamma + N \rightarrow l^+ + l^- + \text{anything}$. The lepton pair l^+l^- may be either electrons or muons. The neutral-current effects in the Bethe-Heitler process⁸⁾ have been investigated by Mikaelian et al.,⁹⁾ in the case of unpolarized photon beams. They have pointed out that the neutral-current contributions to the Bethe-Heitler process give rise to the longitudinal polarizations and the charge asymmetry of the angular distributions for the produced leptons. The observation of the longitudinal polarization of final leptons is, however, rather hard in the experiment. On the other hand, the pure electromagnetic processes, such as two-photon-exchange processes also contribute to yield the charge asymmetry of the angular distributions for final leptons. So, one must eliminate these effects and select only the weak neutral-current contributions towards the Bethe-Heitler process. And very precise measurement are needed for this purpose. For the above reasons, it is rather hard

to examine their results in the experiment. If we keep in mind that high-energy monochromatic and polarized photon beams will be available at the SLAC Hybrid Facility,¹⁰⁾ it is quite significant to study the parity-violating asymmetry for the angular distribution of leptons produced by right- and left-handed photons on various targets.¹¹⁾

The cross sections for the inclusive reactions are larger than those for the exclusive reactions. So, it is natural to expect that the first round of experiments on this reaction is made in the inclusive reactions; $\gamma + N \rightarrow l^+ + l^- + \text{anything}$. Then we at first describe the inclusive lepton pair production with circularly polarized photons on unpolarized targets. For theoretical analysis of inclusive reactions, however, we inevitably use the quark-parton model¹²⁾ to estimate the differential cross sections which are described in terms of nucleon structure functions. In order to give the predictions in a parton model independent way, we also discuss the parity-violating effects in the exclusive lepton pair productions with circularly polarized photons on unpolarized protons; $\gamma + p \rightarrow l^+ + l^- + p$. Although the cross sections for the exclusive reactions are smaller than those for the inclusive reactions, we have the advantage of using the nucleon form factors which are well known in the different experiments¹³⁾ to describe the differential cross sections.

In the evaluation of the photoproduction of lepton pairs, we have found that the main contributions come from the purely electromagnetic Bethe-Heitler processes which are shown in Fig.1. In unified gauge theories, the weak neutral vector boson Z is exchanged as additional contributions shown in Fig.2, and this gives rise to parity non-conservation. From a simple dimensional analysis, these parity-violating effects are generally expected to be of the order $G_F |q^2| / e^2$, for the squared momentum transfer $|q^2| \ll M_Z^2$, where M_Z is the mass of the weak neutral vector boson Z, and G_F and e are the Fermi and electromagnetic

coupling constants, respectively.

There are, of course, other types of processes for the photoproduction of lepton pairs. Figure 3 shows the relevant Feynman diagrams. The contributions of the Compton-type processes are expected to be smaller than those of the Bethe-Heitler processes at high energies of the incoming photons, as is discussed by Mikaelian and Oakes.⁹⁾ Thus, we neglect these diagrams and calculate only the Bethe-Heitler diagrams in Figs.1 and 2.

First we describe a general formulation in §2. We calculate the differential cross section for the lepton pair production with a polarized photon beam on an unpolarized target. In §3, we adopt the Weinberg-Salam model to determine the neutral-current couplings for the purpose of numerical calculations. Section 4 is devoted to the discussion of the inclusive photoproduction of lepton pairs. We define the parity-violating asymmetry of the differential cross sections for lepton produced by right- and left-handed photons for the inclusive reactions. It is expressed in terms of nucleon structure functions. We also discuss its general features and give the numerical results. The exclusive photoproduction of lepton pair is discussed in §5. We also define the parity violating asymmetry of the lepton angular distribution for the exclusive reactions. Numerical results are also given. Conclusions are summarized in §6.

§2. The cross section for lepton pair production with circularly polarized photon beams

In this section, we shall derive the cross section for the process

$$\gamma_\lambda(k) + N(P) \rightarrow l^+(p_+) + l^-(p_-) + X(P') \quad (2.1)$$

where γ_λ , l^+ and l^- are the incoming photon of the helicity λ and the lepton pair, respectively. N and X denote the nucleon target and the possible final states of hadrons such as a single nucleon, one nucleon and one pion and so on. The quantities in parentheses express four-momenta of the corresponding particles and hadronic system.

In what follows, we will use the interaction Lagrangian¹⁴⁾

$$\mathcal{L}_I = e[-\bar{\Psi}\gamma_\mu\Psi + J_\mu^{em}]A^\mu + g_Z[\bar{\Psi}\gamma_\mu(g_V - g_A\gamma_5)\Psi + J_\mu^Z]Z^\mu, \quad (2.2)$$

where Ψ , A_μ and Z_μ stand for the fields of lepton, photon and weak neutral vector boson, respectively. J_μ^{em} and J_μ^Z are the electromagnetic and weak neutral currents of hadrons. e is the proton charge, and g_V , g_A and g_Z are neutral weak coupling constants depending upon gauge models. At present, we leave them free parameters. The interaction (2.2) is also assumed to be time-reversal-invariant. The matrix element mediated by a weak neutral vector boson in Fig.2 can be expressed as

$$\mathcal{M}_Z = \frac{ie g_Z^2}{g^2 - M_Z^2} (g_V j_\alpha - g_A j_\alpha^5) \langle X(P') | J^{Z\alpha}(0) | N(P) \rangle \quad (2.3)$$

where

$$j_\alpha = \epsilon^\mu \bar{u}(p_-) \left[\gamma_\mu \frac{1}{\not{p} - \not{k} - m} \gamma_\alpha + \gamma_\alpha \frac{1}{\not{k} - \not{p}_+ - m} \gamma_\mu \right] v(p_+) \quad (2.4)$$

and

$$j_\alpha^S = \epsilon_\mu \bar{u}(p_-) \left[\gamma_\mu \frac{1}{p_- - k - m} \gamma_\alpha \gamma_5 + \gamma_\alpha \gamma_5 \frac{1}{-p_+ + k - m} \gamma_\mu \right] v(p_+) \quad (2.5)$$

ϵ_μ is the polarization vector of the incident photon, and m is the lepton mass. Similarly, we obtain the electromagnetic matrix element via the Bethe-Heitler mechanism shown in Fig.1

$$M_j = -\frac{ie^3}{g^2} j_\alpha \langle X(P') | J^{em\alpha} | N(P) \rangle \quad (2.6)$$

The cross section for the photoproduction of lepton pairs can be straightforwardly calculated from the matrix elements (2.3) and (2.6). We are interested in the angular distribution of leptons produced by a polarized photon beam on an unpolarized target. Averaging over the initial nucleon spin and summing over all possible final hadronic states, we have the differential cross section for lepton pair production from an unpolarized nucleon:

$$d\sigma = \frac{m^2}{(2\pi)^3 2EE_+E_-} d^3p_+ d^3p_- \frac{1}{2} \sum_{\text{initial nucleon spin}} \sum_{n=1}^{\infty} \sum_{\substack{\text{quantum} \\ \text{numbers} \\ \text{of final hadronic} \\ \text{states}}} \prod_{i=1}^n \int d^3p_i |M_j + M_z|^2 \times (2\pi)^4 \delta^{(4)}(P+k-p_+-p_--P') \quad (2.7)$$

Here, E and E_\pm are the energies of the incident photon and final charged leptons l^\pm , respectively, and $P' = \sum_{i=1}^n p_i$. We have adopted the state normalization as,

$$\langle p, s | p', s' \rangle = \delta^{(3)}(p-p') \delta_{ss'} \quad (2.8)$$

where p and p' are the momenta, and s and s' indicate the spin and other quantum numbers. $\prod_{i=1}^n d^3p_i$ denotes the integration over all the three momenta of the n -body hadron system and the summation should be performed over the possible quantum numbers of the final hadronic states.

Substituting Eqs.(2.3) and (2.6) into Eq.(2.7), we obtain

$$d\sigma = \frac{e^6 m^2 M d^3 p_+ d^3 p_-}{2 (2\pi)^5 E E_+ E_- P_0 g^4} \left[j_\alpha^\dagger j_\beta W^{\alpha\beta} - \frac{g^2 g_z^2}{(g^2 - M_z^2) e^2} (g_{\nu\alpha} j_\nu^\dagger j_\beta - g_{\alpha\nu} j_\nu^\dagger j_\beta^s) R^{\alpha\beta} \right] \quad (2.9)$$

where $q = k - p_+ - p_- = P' - P$ and \dagger denotes the hermitian conjugate. P_0 and M express, respectively, the energy and mass of the target nucleon. The hadronic parts $W^{\alpha\beta}$ and $R^{\alpha\beta}$ are respectively defined by^{15) *}

$$W^{\alpha\beta} = \frac{P_0}{M} \frac{1}{2} \sum_{\substack{\text{initial} \\ \text{nucleon} \\ \text{spin}}} \sum_{n=1}^{\infty} \sum_{\substack{\text{quantum} \\ \text{numbers of} \\ \text{final hadronic} \\ \text{states}}} \prod_{i=1}^n \int d^3 p_i \times \langle N(P) | J^{\dagger em \alpha}_{(0)} | X(P') \rangle \langle X(P') | J^{em \beta}_{(0)} | N(P) \rangle \times (2\pi)^6 \delta^{(4)}(P - P' + q) \quad (2.10)$$

and

$$R^{\alpha\beta} = \frac{P_0}{M} \frac{1}{2} \sum_{\substack{\text{initial} \\ \text{nucleon} \\ \text{spin}}} \sum_{n=1}^{\infty} \sum_{\substack{\text{quantum} \\ \text{numbers of} \\ \text{final hadronic} \\ \text{states}}} \prod_{i=1}^n \int d^3 p_i \left\{ \langle N(P) | J^{\dagger em \alpha}_{(0)} | X(P') \rangle \times \langle X(P') | J^{z\beta}_{(0)} | N(P) \rangle \right. \\ \left. + \langle N(P) | J^{\dagger z\alpha}_{(0)} | X(P') \rangle \langle X(P') | J^{em \beta}_{(0)} | N(P) \rangle \right\} \times (2\pi)^6 \delta^{(4)}(P - P' + q). \quad (2.11)$$

* The definition of $W^{\alpha\beta}$ is different from that of Drell-Walecka by a factor $1/M$.¹⁶⁾

In deriving Eq.(2.9), we have ignored the lepton mass and used the relation $j_\alpha^\dagger j_\beta^5 = j_\alpha^\dagger j_\beta$. The contributions from $|M_z|^2$ have also been ignored. We shall discuss the features of the leptonic and hadronic tensors in the following subsections: 2-1 and 2-2.

2-1. The leptonic tensors

In this subsection we first calculate the leptonic tensors in Eq.(2.7) and discuss their useful properties. Let us consider the case where the polarizations of the final leptons are not measured. Summing over the lepton spins but keeping the photon polarization, we can write

$$\begin{aligned} \sum_{\text{lepton spins}} (j_\alpha^\dagger j_\beta) &= \frac{1}{2} \left[\sum_\lambda \sum_{\text{lepton spins}} (j_\alpha^\dagger j_\beta) + \lambda \sum_{\text{lepton spins}} \{ (j_\alpha^\dagger j_\beta)_{\lambda=1} - (j_\alpha^\dagger j_\beta)_{\lambda=-1} \} \right] \\ &\equiv - \frac{1}{8m^2} (S_{\alpha\beta} + \lambda A_{\alpha\beta}) \end{aligned} \quad (2.12)$$

and

$$\begin{aligned} \sum_{\text{lepton spins}} (j_\alpha^\dagger j_\beta^5) &= \frac{1}{2} \left[\sum_\lambda \sum_{\text{lepton spins}} (j_\alpha^\dagger j_\beta^5) + \lambda \sum_{\text{lepton spins}} \{ (j_\alpha^\dagger j_\beta^5)_{\lambda=1} - (j_\alpha^\dagger j_\beta^5)_{\lambda=-1} \} \right] \\ &\equiv - \frac{1}{8m^2} (S_{\alpha\beta}^5 + \lambda A_{\alpha\beta}^5) \end{aligned} \quad (2.13)$$

where λ is the photon helicity of ± 1 . $S_{\alpha\beta}$ and $S_{\alpha\beta}^5$ are the same as those defined by Mikaelian and Oakes in Ref.9). The tensors $S_{\alpha\beta}$, $A_{\alpha\beta}$, $S_{\alpha\beta}^5$ and $A_{\alpha\beta}^5$ are given by

$$\begin{aligned} S_{\alpha\beta} &= (\varepsilon^\mu \varepsilon^{\dagger\nu} + \varepsilon^{\dagger\mu} \varepsilon^\nu) \text{Tr} \left[\not{P}_+ \left(\gamma_\mu \frac{1}{-P_+ + k} \gamma_\alpha + \gamma_\alpha \frac{1}{P_- - k} \gamma_\mu \right) \not{P}_- \right. \\ &\quad \left. \left(\gamma_\nu \frac{1}{P_- - k} \gamma_\beta + \gamma_\beta \frac{1}{-P_+ + k} \gamma_\nu \right) \right] \end{aligned}$$

$$A_{\alpha\beta} = (\varepsilon^{\mu\nu}\varepsilon^{\rho\sigma} - \varepsilon^{\rho\mu}\varepsilon^{\sigma\nu}) \text{Tr} \left[\not{p}_+ \left(\gamma_\mu \frac{1}{-p_+ + k} \gamma_\alpha + \gamma_\alpha \frac{1}{p_- - k} \gamma_\mu \right) \not{p}_- \right. \\ \left. \left(\gamma_\nu \frac{1}{p_- - k} \gamma_\beta + \gamma_\beta \frac{1}{-p_+ + k} \gamma_\nu \right) \right],$$

$$S_{\alpha\beta}^5 = (\varepsilon^{\mu\nu}\varepsilon^{\rho\sigma} + \varepsilon^{\rho\mu}\varepsilon^{\sigma\nu}) \text{Tr} \left[\gamma_5 \not{p}_+ \left(\gamma_\mu \frac{1}{-p_+ + k} \gamma_\alpha + \gamma_\alpha \frac{1}{p_- - k} \gamma_\mu \right) \not{p}_- \right. \\ \left. \left(\gamma_\nu \frac{1}{p_- - k} \gamma_\beta + \gamma_\beta \frac{1}{-p_+ + k} \gamma_\nu \right) \right]$$

and

$$A_{\alpha\beta}^5 = (\varepsilon^{\mu\nu}\varepsilon^{\rho\sigma} - \varepsilon^{\rho\mu}\varepsilon^{\sigma\nu}) \text{Tr} \left[\gamma_5 \not{p}_+ \left(\gamma_\mu \frac{1}{-p_+ + k} \gamma_\alpha + \gamma_\alpha \frac{1}{p_- - k} \gamma_\mu \right) \not{p}_- \right. \\ \left. \left(\gamma_\nu \frac{1}{p_- - k} \gamma_\beta + \gamma_\beta \frac{1}{-p_+ + k} \gamma_\nu \right) \right] \quad (2.14)$$

where we have neglected the lepton mass. These tensors are the functions of p_\pm and k , and can be easily proved to satisfy the following symmetric or anti-symmetric relations:

$$S_{\alpha\beta}(p_+, p_-) = S_{\beta\alpha}(p_+, p_-) = S_{\alpha\beta}(p_-, p_+),$$

$$S_{\alpha\beta}^5(p_+, p_-) = -S_{\beta\alpha}^5(p_+, p_-) = -S_{\alpha\beta}^5(p_-, p_+),$$

$$A_{\alpha\beta}(p_+, p_-) = -A_{\beta\alpha}(p_+, p_-) = A_{\alpha\beta}(p_-, p_+),$$

$$A_{\alpha\beta}^5(p_+, p_-) = A_{\beta\alpha}^5(p_+, p_-) = -A_{\alpha\beta}^5(p_-, p_+).$$

(2.15)

These relations can be used to discuss the general properties of the cross section and to simplify the following calculations. The explicit formulas of

these tensors are rather lengthy, so that they are not presented here. We list them in Appendix A except for $S_{\alpha\beta}^5$ which does not give a sizable contribution in our case, as will be seen later.

We finally note another important property of the leptonic tensors, which is true only at high energy where the lepton mass can be neglected safely. In such a zero-lepton-mass approximation, the leptonic axial-vector current as well as the vector current is conserved, so that we have

$$\begin{aligned} g^\alpha S_{\alpha\beta} &= 0, & g^\alpha S_{\alpha\beta}^r &= 0, \\ g^\alpha A_{\alpha\beta} &= 0, & g^\alpha A_{\alpha\beta}^r &= 0. \end{aligned} \tag{2.16}$$

These relations are also very useful for us to simplify the contraction of the leptonic and hadronic tensors.

2-2. The hadronic tensors

In this subsection, we discuss the hadronic parts defined in Eq.(2.10) and (2.11). With the aid of the translation operator \mathbb{P} , we can describe

$$J_\mu(x) = e^{iPx} J_\mu(0) e^{-iPx}. \tag{2.17}$$

By making use of this relation, Eqs.(2.10) and (2.11) can be rewritten as follows;

$$W^{\alpha\beta}(g, P) = \frac{(2\pi)^2 P_0}{M} \frac{1}{2} \sum_{\substack{\text{initial} \\ \text{nucleon} \\ \text{spin}}} \int d^4x e^{igx} \langle N(P) | J^{em\alpha}(x) J^{em\beta}(0) | N(P) \rangle \tag{2.18}$$

$$\begin{aligned} R^{\alpha\beta}(g, P) = \frac{(2\pi)^2 P_0}{M} \frac{1}{2} \sum_{\substack{\text{initial} \\ \text{nucleon} \\ \text{spin}}} \int d^4x e^{igx} \langle N(P) | J^{em\alpha}(x) J^{Z\beta}(0) \\ + J^{Z\alpha}(x) J^{em\beta}(0) | N(P) \rangle. \end{aligned} \tag{2.19}$$

Here, we have also used the hermiticity of the electromagnetic and weak neutral currents and the completeness for the states

$$\sum_{n=1}^{\infty} \sum_{\substack{\text{Quantum} \\ \text{numbers of} \\ \text{final hadronic} \\ \text{states}}} \prod_{i=1}^n \int d^3 p_i |\chi(P')\rangle \langle \chi(P')| = 1 \quad (2.20)$$

The expressions (2.18) and (2.19) clearly show that $W^{\alpha\beta}$ and $R^{\alpha\beta}$ are the second rank Lorentz tensors. Moreover, they depend only upon P^μ and q^μ . There are six linearly independent tensors of second rank which can be constructed from P^μ and q^μ . The linearly independent bases used here are presented in Table II. The electromagnetic interaction is parity-conserving and time-reversal-invariant. Also, the electromagnetic current is a conserved one, $\partial^\mu J_\mu^{\text{em}} = 0$. These conditions with the hermiticity mentioned previously imply that $W^{\alpha\beta}$ is a real polar symmetric conserved tensor. On the other hand, the weak interaction is parity-nonconserving and the weak current is not a conserved one, $\partial^\mu J_\mu^Z \neq 0$. The other conditions of time-reversal-invariance of the weak interaction and the hermiticity of the weak current constrain $R^{\alpha\beta}$ to be constructed from real polar symmetric or imaginary axial antisymmetric tensors. Since $R^{\alpha\beta}$ includes the conserved electromagnetic current $J^{\text{em} \mu}$ linearly, we have $q_\alpha q_\beta R^{\alpha\beta} = 0$. Then, making use of the Table II, we obtain the most general forms of $W^{\alpha\beta}$ and $R^{\alpha\beta}$ as

$$W^{\alpha\beta}(q,P) = -W_1 \left(g^{\alpha\beta} - \frac{q^\alpha q^\beta}{q^2} \right) + \frac{W_2}{M^2} \left(P^\alpha - \frac{P \cdot q}{q^2} q^\alpha \right) \left(P^\beta - \frac{P \cdot q}{q^2} q^\beta \right) \quad (2.21)$$

and

$$R^{\alpha\beta}(q,P) = -R_1 \left(q^{\alpha\beta} - \frac{q^\alpha q^\beta}{q^2} \right) + \frac{R_2}{M^2} \left(P^\alpha - \frac{P \cdot q}{q^2} q^\alpha \right) \left(P^\beta - \frac{P \cdot q}{q^2} q^\beta \right) \\ - \frac{iR_3}{2M^2} \epsilon^{\alpha\beta\gamma\delta} P_\gamma q_\delta + \frac{R_4}{M^2} \left(P^\alpha q^\beta + P^\beta q^\alpha - \frac{2P \cdot q}{q^2} q^\alpha q^\beta \right).$$

(2.22)

The structure functions W_i and R_i are scalar functions of q^2 and $P \cdot q$, and are of dimension $(\text{mass})^{-1}$.

2-3. The differential cross sections

The cross section for the lepton pair production with a circularly polarized photon beam on an unpolarized target can be calculated on the basis of Eqs. (2.9) ~ (2.22). Substituting Eqs. (2.10), (2.11), (2.12) and (2.13) into Eq. (2.9), we immediately obtain the difference between the cross section of right- and left-handed photons. The result is

$$d\sigma^{(+)} - d\sigma^{(-)} = \frac{\alpha^3 M d^3p_+ d^3p_-}{\pi^2 E_+ E_-} \frac{g_Z^2}{4E^2(g^2 - M_Z^2)c^2} [g_V A_{\alpha\beta} - g_A A_{\alpha\beta}^5] R^{\alpha\beta}, \quad (2.23)$$

where the (\pm) signs on the cross section indicate positive and negative helicities $\lambda = \pm 1$ of the incoming photon, respectively. Note that $A_{\alpha\beta} W^{\alpha\beta} = 0$, because $A_{\alpha\beta}$ is antisymmetric under the interchange $\alpha \leftrightarrow \beta$, while $W_{\alpha\beta}$ is symmetric (see Eqs. (2.15) and (2.21)).

The sum of the cross sections is clearly given by

$$d\sigma^{(+)} + d\sigma^{(-)} = - \frac{\alpha^3 M d^3p_+ d^3p_-}{\pi^2 E_+ E_-} \frac{1}{4E^2} S_{\alpha\beta} W^{\alpha\beta} + \dots \quad (2.24)$$

where \dots denotes the electromagnetic-weak interference term, including $S_{\alpha\beta}^5 R^{\alpha\beta}$, which can safely be neglected compared with the purely electromagnetic Bethe-Heitler cross section.

We shall now perform the contraction of the leptonic and hadronic tensors in Eqs. (2.23) and (2.24). The terms proportional to q_α and q_β in the hadronic tensors (2.21) and (2.22) vanish owing to the current conservation for lepton (see Eq. (2.16)). Then, we can write

$$S_{\alpha\beta} W^{\alpha\beta} = \frac{-g}{(k \cdot p_+) (k \cdot p_-)} (S_1 W_1 + S_2 W_2) \quad (2.25)$$

and

$$(\partial_\nu A_{\alpha\beta} - \partial_A A_{\alpha\beta}^s) R^{\alpha\beta} = \frac{\delta}{(k \cdot p_+)(k \cdot p_-)} [\partial_\nu A_3 R_3 + \partial_A (A_1 R_1 + A_2 R_2)], \quad (2.26)$$

where S_i and A_i are defined by

$$S_1 = \frac{(k \cdot p_+)(k \cdot p_-)}{\delta} g_{\alpha\beta} S^{\alpha\beta},$$

$$S_2 = - \frac{(k \cdot p_+)(k \cdot p_-)}{\delta} \frac{P_\alpha P_\beta}{M^2} S^{\alpha\beta},$$

$$A_1 = \frac{(k \cdot p_+)(k \cdot p_-)}{\delta} g_{\alpha\beta} A^{s\alpha\beta},$$

$$A_2 = - \frac{(k \cdot p_+)(k \cdot p_-)}{\delta} \frac{P_\alpha P_\beta}{M^2} A^{s\alpha\beta},$$

$$A_3 = \frac{i(k \cdot p_+)(k \cdot p_-)}{\delta} \frac{1}{2M^2} \epsilon_{\alpha\beta\gamma\sigma} P^\gamma \delta^\sigma A^{\alpha\beta}.$$

(2.27)

It is to be noticed here that the other terms do not contribute because of the symmetric or antisymmetric properties (2.15) with respect to the interchange $\alpha \leftrightarrow \beta$.

After simple calculations, we have the explicit formulas of the above products (2.27) in the laboratory system as follows:

$$S_1 = (k \cdot p_+ - p_+ \cdot p_-)^2 + (k \cdot p_- - p_+ \cdot p_-)^2, \quad (2.28)$$

$$S_2 = -S_1/2 + p_+ \cdot p_- \{2E_+ E_- - E(E_+ + E_-)\} \\ + k \cdot p_+ \{EE_+ + E_-(E_- - E_+)\} + k \cdot p_- \{EE_- + E_+(E_+ - E_-)\}, \quad (2.29)$$

$$A_1 = -2E \{ (E_- - p_{\parallel}) - (E_+ - p_{\parallel}) \} [E \{ (E_- - p_{\parallel}) + (E_+ - p_{\parallel}) \} - 2(E_+ E_- - p_{\perp} \cdot p_{\perp} - p_{\parallel} p_{\parallel})] \quad (2.30)$$

$$A_2 = E [2(p_{\parallel} - p_{\parallel})(p_{\perp} \cdot p_{\perp} + p_{\parallel} p_{\parallel}) + 2E_-^2 p_{\parallel} - 2E_+^2 p_{\parallel} + E(-E_-^2 + p_{\parallel}^2 + E_+^2 - p_{\parallel}^2)] \quad (2.31)$$

$$A_3 = \frac{E}{M} [2(p_{\perp} \cdot p_{\perp})^2 - 2(E_+ E_- - p_{\parallel} p_{\parallel}) \{ (E_- - E_+)^2 + (E_+ - p_{\parallel})(E_- - p_{\parallel}) \} + 2p_{\perp} \cdot p_{\perp} \{ (E_- - E_+)^2 + E(E_+ + E_- - p_{\parallel} - p_{\parallel}) - E_- p_{\parallel} - E_+ p_{\parallel} + 2p_{\parallel} p_{\parallel} \} + (E_- - p_{\parallel})^2 E(E_+ E_- - E_+ - 2p_{\parallel}) + (E_+ - p_{\parallel})^2 E(E_+ E_- - E_- - 2p_{\parallel})] \quad (2.32)$$

where the subscripts \parallel and \perp denote the parallel (longitudinal) and perpendicular (transverse) components of momentum with respect to the direction of the photon beam. Note that S_1 , S_2 and A_3 are symmetric under the interchange $p_+ \leftrightarrow p_-$, while A_1 and A_2 are antisymmetric. Hence, A_1 and A_2 vanish for the symmetric pairs $p_+ = p_-$. Then Eqs.(2.23) and (2.24) are written in simple form as,

$$d\sigma^{(+)} - d\sigma^{(-)} = \frac{\alpha^3 d^3p_+ d^3p_-}{\pi^2 E_+ E_-} \frac{g_z^2}{E g^2 (\delta^2 - M_z^2) e^2} \frac{z}{(k \cdot p_+)(k \cdot p_-)} \\ \times [g_V A_3 R_3 + g_A (A_1 R_1 + A_2 R_2)] \quad , \quad (2.33)$$

$$d\sigma^{(+)} + d\sigma^{(-)} = \frac{\alpha^3 d^3p_+ d^3p_-}{\pi^2 E_+ E_-} \frac{1}{E g^4} \frac{z}{(k \cdot p_+)(k \cdot p_-)} (S_1 W_1 + S_2 W_2) \quad . \quad (2.34)$$

§3. The gauge model

Various gauge models make different predictions for the value of the difference between the cross sections of right- and left-handed photons discussed in the previous section. In order to give a numerical estimate of the cross sections, we shall use the standard Weinberg-Salam model⁴⁾ with the Glashow-Iliopoulos-Maiani mechanism,⁵⁾ which determines the neutral-current coupling constants in Eq.(2.2) as,

$$\begin{aligned} g_Z &= \frac{e}{\sin 2\theta_W} , \\ g_V &= -\frac{1}{2} + 2 \sin^2 \theta_W , \\ g_A &= -\frac{1}{2} , \end{aligned} \quad (3.1)$$

where θ_W is the Weinberg angle. The hadronic currents are written in terms of quark fields as follows:

$$J_\mu^{em} = \sum_{\text{quarks}} Q_f \bar{f} \gamma_\mu f \quad (3.2)$$

and

$$J_\mu^Z = \sum_{\text{quarks}} \bar{f} \gamma_\mu (a_f - b_f \gamma_5) f \quad (3.3)$$

with

$$\begin{aligned} Q_u &= Q_c = \frac{2}{3} , & Q_d &= Q_s = -\frac{1}{3} , \\ a_u &= a_c = \frac{1}{2} - \frac{4}{3} \sin^2 \theta_W , \\ a_d &= a_s = -\frac{1}{2} + \frac{2}{3} \sin^2 \theta_W , \\ b_u &= b_c = \frac{1}{2} , & b_d &= b_s = -\frac{1}{2} . \end{aligned}$$

(3.4)

The mass of the weak neutral vector boson Z is related to the Fermi coupling constant G_F as

$$M_Z^2 = \frac{g_Z^2}{\sqrt{2} G_F} .$$

(3.5)

In the numerical calculations we use $\sin^2 \theta_W = 0.23$ for the Weinberg angle which is completely consistent with all the experimental data.³⁾

§4. The inclusive photoproduction of lepton pairs

In this section we shall define the parity violating asymmetry of the differential cross sections for the inclusive photoproduction of lepton pairs. And using the quark-parton model, we give the numerical values of this asymmetry.

4-1. The definition of the parity-violating asymmetry of the cross sections for the inclusive photoproduction of lepton pairs

We are interested in the angular distributions of the leptons produced by left- and right-handed photons on unpolarized proton or deuteron targets, and do not observe the final states of hadrons.

From Eqs.(2.33) and (2.34), we obtain the parity-violating asymmetry of leptons produced by circularly polarized photons for the inclusive reaction:

$$\begin{aligned}
 A(p_+, p_-; k) &= \frac{d\sigma^{(+)} - d\sigma^{(-)}}{d\sigma^{(+)} + d\sigma^{(-)}} \\
 &= \frac{g_Z^2 g^2}{e^2 (g^2 - M_Z^2)} \frac{[g_V A_3 R_3 + g_A (A_1 R_1 + A_2 R_2)]}{(S_1 W_1 + S_2 W_2)}
 \end{aligned}
 \tag{4.1}$$

where the kinematical factors S_i and A_i are explicitly given by Eqs.(2.28)~(2.32), respectively, and the structure functions W_i and R_i are defined in Eqs.(2.21) and (2.22).

We shall now briefly discuss the general features of the above expression (4.1). It is clear from Eq.(2.30) that $A_1 = 0$ for the special configuration, $(k \cdot p_+) = (k \cdot p_-)$, which means, for example, $E_+ = E_-$ and $p_{+\parallel} = p_{-\parallel}$. On the other hand, the explicit formula (2.31) shows that $A_2 = 0$ for either $\underline{p}_{+\perp} = -\underline{p}_{-\perp}$ or $p_{+\parallel} = p_{-\parallel}$ and $|p_{+\perp}| = |p_{-\perp}|$. Therefore, the axial-vector current of lepton does not contribute to the asymmetry (4.1), if we observe only the "azimuthally symmetric" lepton pairs, namely, $E_+ = E_-$, $\theta_+ = \theta_-$, and arbitrary ϕ . Here, θ_{\pm} are, respectively, the polar angles between the final lepton momenta p_{\pm} and the

direction of the incident photon beam, while ϕ is the azimuthal angle between the outgoing lepton pair l^\pm . We emphasize that the above properties are gauge model-independent. In contrast, A_3 in general, does not vanish in such a symmetric case. To estimate the above asymmetry, we further need the knowledge of the nucleon structure functions, W_1, W_2, R_1, R_2 and R_3 .

4-2. Structure functions

We further assume the quark-parton model¹²⁾ to derive the nucleon structure functions. Within the framework of the parton model with spin-1/2 quarks, the Callan-Gross relation⁷⁾ holds not only between W_1 and W_2 but also between R_1 and R_2 :

$$\nu W_2 = 2Mx W_1,$$

$$\nu R_2 = 2Mx R_1,$$

(4.2)

where $\nu = p \cdot q / M$ and the scaling variable $x = -q^2 / 2p \cdot q = -q^2 / 2M\nu$. From the quark currents (3.2) and (3.3), the structure functions are expressed by⁹⁾

$$\nu W_2 = x \sum_{\text{quarks}} Q_f^2 [f(x) + \bar{f}(x)],$$

$$\nu R_2 = 2x \sum_{\text{quarks}} Q_f a_f [f(x) + \bar{f}(x)]$$

and

$$\nu R_3 = -2 \sum_{\text{quarks}} Q_f b_f [f(x) - \bar{f}(x)].$$

(4.3)

Here $q(x)$ and $\bar{q}(x)$ are, respectively, the quark and antiquark distribution functions in the target nucleon.

These distribution functions can be determined from the deep inelastic electron or ν and neutrino scattering data in the same quark-parton picture. Assuming that the sea is SU(3) singlet, Barger and Philips¹⁸⁾ have parametrized them to be

$$\begin{aligned}
 S(x) &= \bar{S}(x) = \bar{u}(x) = \bar{d}(x) = \frac{0.145}{x} (1-x)^9, \\
 u(x) &= \frac{1}{\sqrt{x}} [0.594(1-x^2)^3 + 0.461(1-x^2)^5 + 0.621(1-x^2)^7] + S(x), \\
 d(x) &= \frac{1}{\sqrt{x}} [0.072(1-x^2)^3 + 0.206(1-x^2)^5 + 0.621(1-x^2)^7] + S(x),
 \end{aligned}
 \tag{4.4}$$

for a proton target. The last terms of the above equations for $u(x)$ and $d(x)$ are the contributions from the sea quarks. The distribution functions for a neutron target are given by interchanging $u(x)$ and $d(x)$ in Eq.(4.4). We shall use this parametrization to give numerical values of the asymmetry (4.1).

4-3. Numerical results

We shall first present numerical results for the proton and isoscalar targets in the following configurations:

- (i) $\theta_+ = 15^\circ$, $\theta_- = 5^\circ$, $\phi = 180^\circ$ and $\theta_+ = 10^\circ$, $\theta_- = 5^\circ$, $\phi = 180^\circ$
- (ii) $\theta_+ = \theta_- = 10^\circ$, $\phi = 180^\circ$ and $\theta_+ = \theta_- = 15^\circ$, $\phi = 180^\circ$

at the incident photon energy, $E = 20$ GeV. For each of these configurations, we show the asymmetry as a function of E_- for two energies, $E_+ = 1$ and 5 GeV, in Figs.4,5,6 and 7. For Figs.4 and 6, we give the values for q^2 and x . These values are similar to those for the polarized electron scattering experiments at SLAC⁷⁾.

The asymmetry has also been estimated for $E = 50$ GeV in the same configurations as those of Figs.5 and 7 in order to explore its dependence on the incident photon energy. The results are given for the isoscalar target in Figs.8 and 9. In these numerical calculations, we have used $\sin^2\theta_W = 0.23$ for the Weinberg angle which is completely consistent with all the experimental data³⁾. It is evident from Figs.4 ~ 9 that the parity-violating effects are of the order of 10^{-4} and 10^{-3} for $E = 20$ GeV and 50 GeV, respectively. These effects increase with the angle θ_{\pm} of the observed lepton pair. The same is true for the difference of the asymmetry for the proton and isoscalar targets. However, the differential cross section for the photoproduction of lepton pairs exponentially damps with these polar angles. In Fig.10, for example, we illustrate it as a function of θ_{-} for the fixed angle $\theta_{+} = 5^{\circ}, 10^{\circ}$ and 15° in the case of the incident photon energy of 20 GeV and the isoscalar target. Thus, there is no advantage in setting the angles θ_{\pm} to be so large in the experiment.

For the "azimuthally symmetric" lepton pairs where the axial-vector current of lepton does not contribute, the asymmetry (4.1) vanishes for $\sin^2\theta_W = 1/4$ in the Weinberg-Salam model which gives $g_V = 0$. On the contrary, the vector-like model for charged lepton^{*)} brings about the effects of the order of 10^{-4} for the same Weinberg angle at the incident photon energy of 20 GeV. This feature is shown in Fig.11. We may use it to distinguish the Weinberg-Salam model from the vector-like model of lepton.

* The right-handed electron (or muon) is in a doublet but both u_R and d_R in singlets.

§5. The exclusive photoproduction of lepton pairs

In §4, we have assumed the quark-parton model to give the predictions of the Weinberg-Salam model for the inclusive reaction. In this section we examine the exclusive reaction in order to give the prediction in a parton model independent way. And we shall define the parity-violating asymmetry of the electron (muon) angular distribution for the exclusive lepton production by circularly polarized photons on unpolarized proton targets. In this case we can use the form factors in place of the structure functions for the inclusive reaction, then the predictions are free from the parton model.

5-1. The definition of the parity violating asymmetry of the lepton angular distribution for the exclusive reaction

We now proceed to consider the exclusive lepton pair production with circularly polarized photon beams as,

$$\gamma_{\lambda}(k) + p(P) \rightarrow l^{+}(p_{+}) + l^{-}(p_{-}) + p(P'). \quad (5.1)$$

Here, we specify the initial and final states to proton states in Eq.(2.1). In this case we can derive the matrix elements of the hadronic currents between proton states in terms of the proton form factors as follows:

$$\begin{aligned} \langle p(P') | J_{\alpha}^z(o) | p(P) \rangle &= \frac{M}{(2\pi)^3 \sqrt{P_0 P'_0}} \bar{u}(P') [F_1^z(q^2) \gamma_{\alpha} \\ &+ \frac{i F_2^z(q^2)}{2M} \sigma_{\alpha\beta} q^{\beta} - G_A^z(q^2) \gamma_{\alpha} \gamma_5] u(P) \end{aligned} \quad (5.2)$$

and

$$\begin{aligned} \langle p(P') | J_{\alpha}^{em}(o) | p(P) \rangle &= \frac{M}{(2\pi)^3 \sqrt{P_0 P'_0}} \bar{u}(P') [F_1^{\gamma}(q^2) \gamma_{\alpha} \\ &+ \frac{i F_2^{\gamma}(q^2)}{2M} \sigma_{\alpha\beta} q^{\beta}] u(P) \end{aligned} \quad (5.3)$$

where M is the proton mass. In Eq.(5.2), we have omitted the induced pseudo-scalar form factor because its contribution is negligible for high energies where the lepton mass can safely be ignored. Compton-type diagrams in Fig.3 are also neglected because the perturbation calculation show that their amplitudes are less than 10 percent to those of the Bethe-Heitler processes for the forward production of lepton pairs at the incident photon energy of 20 GeV. The cross section for the process (5.1) can easily be obtained by a simple replacement. The replacement procedures are listed in Appendix B. We are now interested in the angular asymmetry for the lepton produced by circularly polarized photons from unpolarized protons, and we are not concerned with the details of the final states of the proton and the antilepton. Then, integrating over the antilepton variables in Eqs.(2.33) and (2.34), we obtain the differential cross sections for the exclusive lepton pair production of right- and left-handed photons. The results are

$$\begin{aligned}
\frac{d\sigma^{(+)}}{dE_- d\Omega_-} + \frac{d\sigma^{(-)}}{dE_- d\Omega_-} &= \frac{2\alpha^3 E_-}{\pi^2 E(k \cdot p)} \int d\Omega_+ \frac{ME_+}{P_0'(k \cdot p_+) g^4} \\
&\times \left[-S_1 \frac{g^2}{4M^2} \{G_{M,p}^\sigma(g^2)\}^2 \right. \\
&\left. + S_2 \frac{1}{(1 - \frac{g^2}{4M^2})} \left\{ (G_{E,p}^\sigma(g^2))^2 - \frac{g^2}{4M^2} (G_{M,p}^\sigma(g^2))^2 \right\} \right]
\end{aligned} \tag{5.4}$$

and

$$\frac{d\sigma^{(+)}}{dE_- d\Omega_-} - \frac{d\sigma^{(-)}}{dE_- d\Omega_-} = -\frac{\alpha^2 g_z^2 E_-}{\pi^3 E(k \cdot p)} \int d\Omega_+ \frac{ME_+}{P_0'(k \cdot p_+) g^2 (g^2 - M_z^2)}$$

$$\begin{aligned}
& \times \left[-g_V A_3 G_{M,p}^\gamma(q^2) G_{A,p}^Z(q^2) \right. \\
& \quad + g_A \left\{ -A_1 \frac{q^2}{4M^2} G_{M,p}^\gamma(q^2) G_{M,p}^Z(q^2) \right. \\
& \quad \left. \left. + A_2 \frac{1}{1 - \frac{q^2}{4M^2}} \left(G_{E,p}^\gamma(q^2) G_{E,p}^Z(q^2) - \frac{q^2}{4M^2} G_{M,p}^\gamma(q^2) G_{M,p}^Z(q^2) \right) \right\} \right]
\end{aligned} \tag{5.5}$$

where

$$E_+ = \frac{M(E_- - E) + EE_-(1 - \cos\theta_-)}{E_- \{ 1 - \cos\theta_+ \cos\theta_- - \sin\theta_+ \sin\theta_- \cos(\phi_+ - \phi_-) - E(1 - \cos\theta_+) - M \}}, \tag{5.6}$$

$$P'_+ = M + E - E_+ - E_-, \tag{5.7}$$

$$q^2 = -2M(E - E_- - E_+). \tag{5.8}$$

Here, $G_E(q^2)$ and $G_M(q^2)$ are the Sachs electric and magnetic form factors and defined by¹⁹⁾

$$G_E(q^2) = F_1(q^2) + \frac{q^2}{4M^2} F_2(q^2) \tag{5.9}$$

and

$$G_M(q^2) = F_1(q^2) + F_2(q^2). \tag{5.10}$$

The superscripts γ and Z imply the form factors of the electromagnetic and weak neutral currents, respectively, while the subscript p indicates the proton form factors in Eqs.(5.4) and (5.5). From Eqs.(5.4) and (5.5), we define the parity-violating asymmetry of the electron (muon) angular distribution for the exclusive lepton production by right- and left-handed photons on proton target:

$$A(p; k) = \left[\frac{d\sigma^{(+)}}{dE_- d\Omega_-} - \frac{d\sigma^{(-)}}{dE_- d\Omega_-} \right] / \left[\frac{d\sigma^{(+)}}{dE_- d\Omega_-} + \frac{d\sigma^{(-)}}{dE_- d\Omega_-} \right]. \tag{5.11}$$

In our numerical estimate of the asymmetry, we cut off the antilepton energy lower than 1 GeV in practice.

5-2. Form factors

For the estimation of the cross section of the exclusive reaction we are now in a position to discuss the form factors for the hadronic currents.

Neglecting the contribution of the strange and charmed quarks in the nucleon, the form factors of the neutral vector current can be related to the electromagnetic form factors of nucleons through the isospin property.²⁰⁾ From Eqs. (3.2) ~ (3.4), we have

$$G_{E,p}^z(q^2) = \frac{1}{2} [G_{E,p}^{\gamma}(q^2) - G_{E,n}^{\gamma}(q^2)] - 2 \sin^2 \theta_W G_{E,p}^{\gamma}(q^2),$$

and

$$G_{M,p}^z(q^2) = \frac{1}{2} [G_{M,p}^{\gamma}(q^2) - G_{M,n}^{\gamma}(q^2)] - 2 \sin^2 \theta_W G_{M,p}^{\gamma}(q^2).$$

(5.12)

for the Weinberg-Salam model. The subscript n(p) indicates the neutron (proton) form factors. In a similar manner, we obtain for the neutral axial-vector current²⁰⁾

$$G_{A,p}^z(q^2) = \frac{1}{2} g_A(q^2)$$

(5.13)

where $g_A(q^2)$ is the axial-vector form factor for the neutron β decay. On the other hand, the electromagnetic form factors G_E^{γ} and G_M^{γ} are well known experimentally at least for low energies, and they have the same dipole q^2 dependence:

$$G_{E,p}^{\gamma}(q^2) = \frac{G_{M,p}^{\gamma}(q^2)}{1 + \mu_p} = \frac{G_{M,n}^{\gamma}(q^2)}{\mu_n} = \left(1 - \frac{q^2}{0.71(\text{GeV})^2} \right)^{-2},$$

$$G_{E,n}^{\gamma}(q^2) \approx 0,$$

(5.14)

where $\mu_p = 1.79$ and $\mu_n = -1.91$ are the proton and neutron anomalous magnetic moments, respectively.²¹⁾ Similarly, we take the axial-vector form factor of the dipole form

$$g_A(q^2) = g_A(0) \left(1 - \frac{q^2}{M_A^2} \right)^{-2} \quad (5.15)$$

where $g_A(0) = 1.253 \pm 0.007$ is the axial-vector coupling constant for the neutron β decay.²²⁾ The parameter M_A is determined by the pseudo-elastic neutrino reaction¹³⁾ but it is not so well settled yet. In our numerical calculations, we take $M_A^2 = 0.90 \text{ GeV}^2$. It is, however, noted here that our numerical results for the asymmetries are scarcely affected by the value of M_A^2 so far as it ranges from 0.71 GeV^2 to 1.10 GeV^2 , compatible with the experiments.

5-3. Numerical results

We shall present the numerical results of the asymmetry in the following configurations:

- (i) $E = 10 \text{ GeV}, \quad \theta_- = 1^\circ, 5^\circ,$
- (ii) $E = 20 \text{ GeV}, \quad \theta_- = 1^\circ, 5^\circ, 10^\circ,$
- (iii) $E = 50 \text{ GeV}, \quad \theta_- = 5^\circ, 10^\circ.$

In Figs.12 ~ 18, the asymmetry is shown as a function of the outgoing lepton energy E_- . The Weinberg angle is the same as in §4. In the case of the incident photon energy, $E = 10 \text{ GeV}$, we find the parity-violating asymmetries to be of the order of 10^{-9} and 10^{-7} for the lepton production angle $\theta_- = 1^\circ$ and 5° . For $E = 20 \text{ GeV}$, the asymmetries are of the order of 10^{-7} , 10^{-6} and 10^{-5} for $\theta_- = 1^\circ, 5^\circ$ and 10° , respectively, while for $E = 50 \text{ GeV}$, they are of the order of 10^{-5} and 10^{-4} for $\theta_- = 5^\circ$ and 10° . The parity-violating effects clearly increase with the angle θ_- of the observed lepton. However, the differential cross section

for the photoproduction of lepton pairs exponentially damps with this angle and also with the lepton energy E_- . In Fig.19, for example, we illustrate it as a function of E_- for the fixed angles $\theta_- = 1^\circ, 5^\circ$ and 10° in the case of $E = 20$ GeV. Thus, similar to the inclusive reaction, there is no advantage in setting the angle θ_- to be so large in the experiment. In the above numerical estimates, we have cut off the antilepton energy lower than 1 GeV, as was previously mentioned. In fact, this cut-off may be removed, because it makes no visible difference in our numerical results as far as they are shown in Figs.12 ~ 19. Of course, it does affect the behavior near at the maximum energy of the lepton.

§6. Conclusions

A. We find that the parity-violating asymmetry is of the order of 10^{-4} for the inclusive lepton pair production with circularly polarized photons on unpolarized isoscalar and proton targets at the incident photon energy of 20 GeV. It has also been estimated to be of the order of 10^{-3} for $E = 50$ GeV in order to show its dependence on the incident photon energy E . We point out that the observation of the "azimuthally symmetric" lepton pairs production may be used to draw the information of a g_V coupling constant independently on that of a g_A coupling constant. As an example, we show that it can be used to distinguish the Weinberg-Salam model from the vector-like model for charged lepton.

B. It is evident from Figs.14 and 15 that the parity-violating asymmetry is of the order of $10^{-7} \sim 10^{-5}$ for the exclusive lepton pair production with circularly polarized photons on unpolarized proton targets at the incident photon energy of 20 GeV in the lepton production angle range from 1° to 10° . The exclusive photoproduction is useful to determine the relevant form of the electron- and the muon-quark neutral current couplings without using the quark-parton model. This is entirely because we can use the nucleon form factors at the proton vertex. Since the form factors are established in a wide energy range of the incident particles, the lower incident energy is available for this reaction. We show in Figs.12 and 13 the parity-violating asymmetry at the incident photon energy of 10 GeV by way of example.

C. Finally, we shall briefly remark the feasibility of observing the above neutral-current effects. The monochromatic and polarized photon beam of 20 GeV will be available at SLAC in the near future.¹⁰⁾ Given the rapid experimental progress taking place in this field at the present time, we can reasonably expect that it will be feasible to observe the parity-violating asymmetry in the photoproduction of lepton pairs. These lepton pairs which we discuss in this thesis may be the electrons and the muons. Such measurements are quite useful for the determination of the electron- and the muon-quark neutral-current couplings.

Acknowledgement

The author is greatly indebted to Professor M. Morita for constant guidance and encouragements. He would like to express his sincere thanks to Professor Y. Yokoo who suggested this problem and offered many invaluable advices throughout this work, and to Mr. K. Ushio for stimulating discussions. Finally, he would like to express his appreciation to Mr. K. Konashi for his aid of making computer-codes and Mrs. Hisayo Konashi for beautiful typing.

Appendix A

We shall present the explicit formulas of the leptonic tensors encountered in §2. In Eqs.(2.12) and (2.13), we define;

$$S_{\alpha\beta} = -4m^2 \sum_{\lambda} \sum_{\substack{\text{lepton} \\ \text{spins}}} (j_{\alpha}^{\dagger} j_{\beta}) \quad (\text{A.1})$$

$$S_{\alpha\beta}^5 = -4m^2 \sum_{\lambda} \sum_{\substack{\text{lepton} \\ \text{spins}}} (j_{\alpha}^{\dagger} j_{\beta}^5) \quad (\text{A.2})$$

$$A_{\alpha\beta} = -4m^2 \sum_{\substack{\text{lepton} \\ \text{spins}}} [(j_{\alpha}^{\dagger} j_{\beta})_{\lambda=1} - (j_{\alpha}^{\dagger} j_{\beta})_{\lambda=-1}] \quad (\text{A.3})$$

$$A_{\alpha\beta}^5 = -4m^2 \sum_{\substack{\text{lepton} \\ \text{spins}}} [(j_{\alpha}^{\dagger} j_{\beta}^5)_{\lambda=1} - (j_{\alpha}^{\dagger} j_{\beta}^5)_{\lambda=-1}]. \quad (\text{A.4})$$

From Eqs.(A.1) and (A.2), one finds that $S_{\alpha\beta}$ and $S_{\alpha\beta}^5$ are the same as those defined by Mikaelian and Oakes.⁹⁾ After tedious but straightforward calculations, we have

$$\begin{aligned} S_{\alpha\beta} = \frac{-4}{(p_+ \cdot k)(p_- \cdot k)} [& -g_{\alpha\beta} \{ (p_+ \cdot p_- - p_+ \cdot k)^2 + (p_+ \cdot p_- - p_- \cdot k)^2 \} \\ & + (p_{+\alpha} p_{-\beta} + p_{+\beta} p_{-\alpha}) (2p_+ \cdot p_- - k \cdot p_- - k \cdot p_+) \\ & + (p_{+\alpha} k_{\beta} + p_{+\beta} k_{\alpha}) (p_+ \cdot k - p_+ \cdot p_-) \\ & + (p_{-\alpha} k_{\beta} + p_{-\beta} k_{\alpha}) (p_- \cdot k - p_+ \cdot p_-) \\ & + 2p_+ \cdot k p_{-\alpha} p_{-\beta} + 2p_- \cdot k p_{+\alpha} p_{+\beta} \quad], \end{aligned} \quad (\text{A.5})$$

$$\begin{aligned} A_{\alpha\beta} = -4 \left(\frac{p_+ \cdot \varepsilon^{\dagger}}{p_+ \cdot k} - \frac{p_- \cdot \varepsilon^{\dagger}}{p_- \cdot k} \right) [& \frac{1}{p_+ \cdot k} \{ p_- \cdot \varepsilon (p_{+\beta} k_{\alpha} - p_{+\alpha} k_{\beta}) + p_- \cdot k (p_{+\alpha} \varepsilon_{\beta} - p_{+\beta} \varepsilon_{\alpha}) \\ & - p_+ \cdot p_- (k_{\alpha} \varepsilon_{\beta} - \varepsilon_{\alpha} k_{\beta}) \} \\ & + \frac{1}{p_- \cdot k} \{ p_+ \cdot \varepsilon (p_{-\beta} k_{\alpha} - p_{-\alpha} k_{\beta}) + p_+ \cdot k (p_{-\beta} \varepsilon_{\alpha} - p_{-\alpha} \varepsilon_{\beta}) \\ & - p_+ \cdot p_- (\varepsilon_{\alpha} k_{\beta} - \varepsilon_{\beta} k_{\alpha}) \}] \end{aligned}$$

$$\begin{aligned}
& -4 \left(\frac{P_+ \cdot \varepsilon}{P_+ \cdot k} - \frac{P_- \cdot \varepsilon}{P_- \cdot k} \right) \left[\frac{1}{P_- \cdot k} \left\{ P_+ \cdot \varepsilon^\dagger (P_- \cdot k_\alpha - P_- \cdot k_\beta) + P_+ \cdot k (P_- \cdot \varepsilon_\beta^\dagger - P_- \cdot \varepsilon_\alpha^\dagger) \right. \right. \\
& \quad \left. \left. - P_+ \cdot P_- (\varepsilon_\beta^\dagger k_\alpha - \varepsilon_\alpha^\dagger k_\beta) \right\} \right. \\
& \quad \left. + \frac{1}{P_+ \cdot k} \left\{ P_- \cdot \varepsilon^\dagger (P_+ \cdot k_\beta - P_+ \cdot k_\alpha) - P_- \cdot k (P_+ \cdot \varepsilon_\alpha^\dagger - P_+ \cdot \varepsilon_\beta^\dagger) \right. \right. \\
& \quad \left. \left. - P_+ \cdot P_- (\varepsilon_\alpha^\dagger k_\beta - \varepsilon_\beta^\dagger k_\alpha) \right\} \right] \\
& -4 \left[\frac{1}{P_+ \cdot k} \left\{ P_- \cdot k (\varepsilon_\alpha^\dagger \varepsilon_\beta - \varepsilon_\alpha \varepsilon_\beta^\dagger) + P_- \cdot \varepsilon (k_\alpha \varepsilon_\beta^\dagger - k_\beta \varepsilon_\alpha^\dagger) + P_- \cdot \varepsilon^\dagger (k_\beta \varepsilon_\alpha - k_\alpha \varepsilon_\beta) \right\} \right. \\
& \quad \left. + \frac{1}{P_- \cdot k} \left\{ P_+ \cdot k (\varepsilon_\alpha^\dagger \varepsilon_\beta - \varepsilon_\alpha \varepsilon_\beta^\dagger) + P_+ \cdot \varepsilon^\dagger (\varepsilon_\alpha k_\beta - \varepsilon_\beta k_\alpha) + P_+ \cdot \varepsilon (\varepsilon_\beta^\dagger k_\alpha - \varepsilon_\alpha^\dagger k_\beta) \right\} \right],
\end{aligned}$$

(A.6)

$$\begin{aligned}
A_{\alpha\beta}^5 = & -4i \left[\left(\frac{-P_+ \cdot \varepsilon}{P_+ \cdot k} + \frac{P_- \cdot \varepsilon}{P_- \cdot k} \right) \frac{1}{P_- \cdot k} \left\{ P_{+\alpha} \varepsilon_{\mu\nu\rho\beta} k^\mu P_+^\nu \varepsilon^{\rho\sigma} + P_{-\beta} \varepsilon_{\mu\nu\rho\alpha} k^\mu P_-^\nu \varepsilon^{\rho\sigma} \right. \right. \\
& \quad \left. \left. + g_{\alpha\beta} \varepsilon_{\mu\nu\rho\sigma} k^\mu P_+^\nu P_-^\rho \varepsilon^{\sigma\kappa} \right\} \right. \\
& - \left(\frac{-P_+ \cdot \varepsilon^\dagger}{P_+ \cdot k} + \frac{P_- \cdot \varepsilon^\dagger}{P_- \cdot k} \right) \frac{1}{P_+ \cdot k} \left\{ P_{-\alpha} \varepsilon_{\mu\nu\rho\beta} k^\mu P_-^\nu \varepsilon^{\rho\sigma} + P_{-\beta} \varepsilon_{\mu\nu\rho\alpha} k^\mu P_-^\nu \varepsilon^{\rho\sigma} \right. \\
& \quad \left. + g_{\alpha\beta} \varepsilon_{\mu\nu\rho\sigma} k^\mu P_+^\nu P_-^\rho \varepsilon^{\sigma\kappa} \right\} \\
& + \left(\frac{-P_+ \cdot \varepsilon}{P_+ \cdot k} + \frac{P_- \cdot \varepsilon}{P_- \cdot k} \right) \frac{1}{P_- \cdot k} \left\{ P_{+\alpha} \varepsilon_{\mu\nu\rho\beta} k^\mu P_-^\nu \varepsilon^{\rho\sigma} + P_{+\beta} \varepsilon_{\mu\nu\rho\alpha} k^\mu P_-^\nu \varepsilon^{\rho\sigma} \right. \\
& \quad \left. - g_{\alpha\beta} \varepsilon_{\mu\nu\rho\sigma} k^\mu P_+^\nu P_-^\rho \varepsilon^{\sigma\kappa} \right\} \\
& - \left(\frac{-P_+ \cdot \varepsilon^\dagger}{P_+ \cdot k} + \frac{P_- \cdot \varepsilon^\dagger}{P_- \cdot k} \right) \frac{1}{P_+ \cdot k} \left\{ P_{+\alpha} \varepsilon_{\mu\nu\rho\beta} k^\mu P_-^\nu \varepsilon^{\rho\sigma} + P_{+\beta} \varepsilon_{\mu\nu\rho\alpha} k^\mu P_-^\nu \varepsilon^{\rho\sigma} \right. \\
& \quad \left. - g_{\alpha\beta} \varepsilon_{\mu\nu\rho\sigma} k^\mu P_+^\nu P_-^\rho \varepsilon^{\sigma\kappa} \right\} \\
& + \frac{1}{P_+ \cdot k} \left\{ -P_{+\alpha} \varepsilon_{\mu\nu\rho\beta} k^\mu \varepsilon^\nu \varepsilon^{\rho\sigma} - P_{-\beta} \varepsilon_{\mu\nu\rho\alpha} k^\mu \varepsilon^\nu \varepsilon^{\rho\sigma} + g_{\alpha\beta} \varepsilon_{\mu\nu\rho\sigma} k^\mu P_-^\nu \varepsilon^{\rho\sigma} \varepsilon^{\tau\kappa} \right\} \\
& + \frac{1}{P_- \cdot k} \left\{ P_{+\alpha} \varepsilon_{\mu\nu\rho\beta} k^\mu \varepsilon^\nu \varepsilon^{\rho\sigma} + P_{+\beta} \varepsilon_{\mu\nu\rho\alpha} k^\mu \varepsilon^\nu \varepsilon^{\rho\sigma} - g_{\alpha\beta} \varepsilon_{\mu\nu\rho\sigma} k^\mu P_+^\nu \varepsilon^{\rho\sigma} \varepsilon^{\tau\kappa} \right\} \Big].
\end{aligned}$$

(A.7)

Here, ϵ is the photon polarization vector corresponding to the helicity 1. In the coordinate system where Z axis is along the direction of the incoming photon, ϵ is explicitly given by

$$\mathcal{E} = \frac{1}{\sqrt{2}} (0, 1, i, 0). \quad (\text{A.8})$$

We have not listed the expression of $S_{\alpha\beta}^5$ since it does not give a sizable contribution to the asymmetry (4.1) as was already mentioned in §2. The explicit formulas (A.5), (A.6) and (A.7), for leptonic tensors show the symmetric or antisymmetric properties given in Eq.(2.15) clearly.

Appendix B

For the exclusive photoproduction of lepton pairs, we specify the final states to the proton one in Eqs.(2.10) and (2.11). Using Eqs.(5.2) and (5.3), we can express $W^{\alpha\beta}$ and $R^{\alpha\beta}$ in terms of the Sachs form factors,

$$\begin{aligned}
 W_{\text{proton}}^{\alpha\beta}(\delta, P) &= \frac{1}{2} \sum_{\substack{\text{initial} \\ \text{final} \\ \text{proton} \\ \text{spins}}} \frac{P_0}{M} \int d^3P' \langle p(P) | J_{(0)}^{\dagger\alpha} | p(P') \rangle \langle p(P') | J_{(0)}^{\alpha\beta} | p(P) \rangle \\
 &\quad \times (2\pi)^6 \delta^{(4)}(P - P' + \delta) \\
 &= \frac{\delta(M - P_0' + \delta_0)}{4P_0' M} \left[(G_M^\gamma(\delta^2))^2 \delta^2 g^{\alpha\beta} + \frac{4}{(1 - \frac{\delta^2}{4M^2})} \left\{ (G_E^\gamma(\delta^2))^2 - \frac{\delta^2}{4M^2} (G_M^\gamma(\delta^2))^2 \right\} \right. \\
 &\quad \left. \times \left(P^\alpha - \frac{P \cdot \delta}{\delta^2} \delta^\alpha \right) \left(P^\beta - \frac{P \cdot \delta}{\delta^2} \delta^\beta \right) \right],
 \end{aligned}$$

$$\begin{aligned}
 R_{\text{proton}}^{\alpha\beta}(\delta, P) &= \frac{1}{2} \sum_{\substack{\text{initial} \\ \text{final} \\ \text{proton} \\ \text{spins}}} \frac{P_0}{M} \int d^3P' \left\{ \langle p(P) | J_{(0)}^{\dagger\alpha} | p(P') \rangle \langle p(P') | J_{(0)}^{\beta} | p(P) \rangle \right. \\
 &\quad \left. + \langle p(P) | J_{(0)}^{\dagger\alpha} | p(P') \rangle \langle p(P') | J_{(0)}^{\alpha\beta} | p(P) \rangle \right\} \\
 &\quad \times (2\pi)^6 \delta^{(4)}(P - P' + \delta) \\
 &= \frac{2\delta(M - P_0' + \delta_0)}{4P_0' M} \left[G_M^\gamma(\delta^2) G_M^z(\delta^2) \delta^2 g^{\alpha\beta} \right. \\
 &\quad \left. + \frac{4}{(1 - \frac{\delta^2}{4M^2})} \left\{ G_E^\gamma(\delta^2) G_E^z(\delta^2) - \frac{\delta^2}{4M^2} G_M^\gamma(\delta^2) G_M^z(\delta^2) \right\} \right. \\
 &\quad \left. \times \left(P^\alpha - \frac{P \cdot \delta}{\delta^2} \delta^\alpha \right) \left(P^\beta - \frac{P \cdot \delta}{\delta^2} \delta^\beta \right) \right. \\
 &\quad \left. + 2i G_M^\gamma(\delta^2) G_M^z(\delta^2) \epsilon^{\alpha\beta\rho\sigma} P_\rho \delta_\sigma \right].
 \end{aligned}$$

Correspondences between these equations and Eqs.(2.21) and (2.22) gives the differential cross sections of the exclusive lepton pair production by the following substitutions in Eqs.(2.33) and (2.34),

$$W_1 \rightarrow - \frac{g^2}{4MP_0'} (G_M^\sigma(q^2))^2 \delta(M-P_0'+q_0), \quad (\text{B.1})$$

$$W_2 \rightarrow \frac{M}{P_0' \left(1 - \frac{g^2}{4M^2}\right)} \left[(G_E^\sigma(q^2))^2 - \frac{g^2}{4M^2} (G_M^\sigma(q^2))^2 \right] \delta(M-P_0'+q_0), \quad (\text{B.2})$$

$$R_1 \rightarrow - \frac{2g^2}{4MP_0'} G_M^\sigma(q^2) G_M^z(q^2) \delta(M-P_0'+q_0), \quad (\text{B.3})$$

$$R_2 \rightarrow \frac{2M}{P_0' \left(1 - \frac{g^2}{4M^2}\right)} \left[G_E^\sigma(q^2) G_E^z(q^2) - \frac{g^2}{4M^2} G_M^\sigma(q^2) G_M^z(q^2) \right] \delta(M-P_0'+q_0), \quad (\text{B.4})$$

$$R_3 \rightarrow - \frac{2M}{P_0'} G_M^\sigma(q^2) G_A^z(q^2) \delta(M-P_0'+q_0). \quad (\text{B.5})$$

References

- 1) F. J. Hasert et al., Phys. Letters 46B(1973), 138.
A. Benvenuti et al., Phys. Rev. Letters 32(1974), 800.
B. C. Barish et al., Phys. Rev. Letters 34(1975), 538.
- 2) S. J. Barish et al., Phys. Rev. Letters 33(1974), 448.
W. Lee et al., Phys. Rev. Letters 38(1977), 202.
- 3) C. Baltay, Proceeding of the 19th International Conference on High energy Physics, Tokyo, 1978, edited by S. Homma, M. Kawaguchi and H. Miyazawa, p.882.
- 4) S. Weinberg, Phys. Rev. Letters 19(1967), 1264.
A. Salam, Elementary Particle Theory, edited by N. Svartholm (Almqvist and Wiksell, Stockholm, 1968), p.367.
- 5) S. L. Glashow, J. Illiopoulos and L. Maiani, Phys. Rev. D2(1970), 1285.
- 6) L. L. Lewis et al., Phys. Rev. Letters 39(1977), 795.
P. E. G. Baird et al., Phys. Rev. Letters 39(1977), 798.
L. M. Barkov and M. S. Zolotorev, JETP Letters 27(1978), 357;
Phys. Letters 85B(1979), 308.
- 7) C. Y. Prescott et al., Phys. Letters 77B(1978), 347;
Phys. Letters 84B(1979), 524.
- 8) Y. S. Tsai, Rev. Mod. Phys. 46(1974), 815.
- 9) K. O. Mikaelian and R. J. Oakes, Phys. Rev. Letters 70B(1977), 358;
Phys. Rev. D16(1977), 3216.
R. F. Cahalan and K. O. Mikaelian, Phys. Rev. D10(1974), 3769.
- 10) J. Ballam et al., Proposal report, SLAC, Oct. 1978.
- 11) Y. Yokoo, H. Konashi and K. Ushio, Phys. Letters 87B(1979), 61.
H. Konashi, K. Ushio and Y. Yokoo, Prog. Theor. Phys. 62(1979), 1062.
H. Konashi, K. Ushio and Y. Yokoo, to be published.

- 12) See, for example, R. P. Feynman, Photon-Hadron Interactions (Benjamin, Reading, Mass., 1972).
- 13) P. Musset and J-P Vialle, Phys. Reports 39C(1978),1.
 J. Steinberger, Lectures given at CERN School of Physics, Wepion, Belgium, 1976.
 D. H. Perkins, Proceedings of the 1975 International Symposium on Lepton and Photon Interactions at High Energies, Stanford, California, 1975, edited by W. T. Kirk, p. 571.
- 14) The conventions for metric, Dirac equation, etc. are those of J. D. Bjorken and S. D. Drell, Relativistic Quantum Fields (McGraw-Hill, New York, 1965). In ref. 11), the Pauli-Dirac metric and conventions are used. The comparison between these metrics are described in H. Pietschmann, Formulae and Results in Weak Interactions (Springer-Verlag, Wien New York, 1974), p.61.
- 15) E. Derman, Phys. Rev. D7(1973), 2755.
- 16) S. D. Drell and J. D. Walecka Ann. of Phys. 28(1964), 18.
- 17) C. G. Callan and D. J. Gross, Phys. Rev. Letters 22(1969), 156.
- 18) V. Barger and R. J. N. Phillips, Nucl. Phys. B73(1974), 269
- 19) F. J. Ernst, R. G. Sachs and K. C. Wali, Phys. Rev. 119(1960), 1105.
 R. G. Sachs, Phys. Rev. 126(1962), 2256.
- 20) S. M. Bilenky, N. A. Dadajan and E. H. Hristova, Sov. J. Nucl. Phys. 21(1976), 657.
 R. N. Cahn and F. J. Gilman, Phys. Rev. D17(1978), 1313.
 F. J. Gilman and T. Tsao, Phys. Rev. D19(1979), 790.
 E. Ch. Christova and S. T. Petcov, Phys. Letters 84B(1979), 250.
- 21) M. Gourdin, Phys. Reports, 11C(1974), 29.
- 22) Particle Data Group, Phys. Letters 75B(1978), 4.

Figure captions

Fig. 1. Feynman diagrams for the photoproduction of lepton pairs mediated by a photon.

Fig. 2. Feynman diagrams for the photoproduction of lepton pairs mediated by a weak neutral vector boson.

Fig. 3. Compton-type electromagnetic (a) and weak (b) amplitudes for lepton pair production.

Fig. 4. The asymmetry A as a function of E_- for $\theta_+ = 5^\circ$, $\theta_- = 15^\circ$, $\phi = 180^\circ$ and $E = 20$ GeV. The asymmetry is given in units of 10^{-4} for the Weinberg-Salam model with $\sin^2\theta_W = 0.23$. The solid and dash-dotted curves correspond to the isoscalar and proton targets, respectively for $E_+ = 5$ GeV. The dashed curve corresponds to $E_+ = 1$ GeV for the isoscalar and proton targets. At the energy of $E_+ = 1$ GeV, these two curves are so close each other that we could not draw them distinctively. Here, the values of q^2 and x are as follows;

$$E_+ = 1 \text{ GeV}, E_- = 1 \text{ GeV} \quad q^2 = -1.395(\text{GeV}/c)^2 \quad x = 0.041$$

$$E_- = 10 \text{ GeV} \quad q^2 = -1.679(\text{GeV}/c)^2 \quad x = 0.099$$

$$E_+ = 5 \text{ GeV}, E_- = 1 \text{ GeV} \quad q^2 = -6.364(\text{GeV}/c)^2 \quad x = 0.242$$

$$E_- = 10 \text{ GeV} \quad q^2 = -2.306(\text{GeV}/c)^2 \quad x = 0.246$$

Fig. 5. The asymmetry A as a function of E_- for $\theta_+ = 10^\circ$, $\theta_- = 5^\circ$, $\phi = 180^\circ$ and $E = 20$ GeV. The asymmetry is given in units of 10^{-4} for the Weinberg-Salam model with $\sin^2\theta_W = 0.23$. The solid and dashed curves correspond to $E_+ = 5$ and 1 GeV, respectively, for the isoscalar target. The dash-dotted and dash-double-dotted curves correspond to the same for the proton target. Below $E_- = 4$ GeV, the dash-double-

dotted line is so close to the dashed one that we could not draw it distinctively.

Fig. 6. The asymmetry A in units of 10^{-4} as a function of E_- for $\theta_+ = \theta_- = 10^\circ$, $\phi = 180^\circ$ and $E = 20$ GeV, in the Weinberg-Salam model with $\sin^2 \theta_W = 0.23$. Notation is the same as in Fig. 5. Here, the values of q^2 and x are as follows;

$$\begin{aligned} E_+ = 1 \text{ GeV}, E_- = 1 \text{ GeV} \quad q^2 = -1.095(\text{GeV}/c)^2 \quad x = 0.032 \\ E_- = 10 \text{ GeV} \quad q^2 = -5.478(\text{GeV}/c)^2 \quad x = 0.324 \end{aligned}$$

$$\begin{aligned} E_+ = 5 \text{ GeV}, E_- = 1 \text{ GeV} \quad q^2 = -3.043(\text{GeV}/c)^2 \quad x = 0.116 \\ E_- = 10 \text{ GeV} \quad q^2 = -3.085(\text{GeV}/c)^2 \quad x = 0.329 \end{aligned}$$

Fig. 7. The asymmetry A in units of 10^{-4} as a function of E_- for $\theta_+ = \theta_- = 15^\circ$, $\phi = 180^\circ$ and $E = 20$ GeV, in the Weinberg-Salam model with $\sin^2 \theta_W = 0.23$. Notation is the same as in Fig. 5.

Fig. 8. The asymmetry A as a function of E_- for $\theta_+ = 10^\circ$, $\theta_- = 5^\circ$, $\phi = 180^\circ$ and $E = 50$ GeV. The asymmetry is given in units of 10^{-4} for the Weinberg-Salam model with $\sin^2 \theta_W = 0.23$. The solid and dashed curves are, respectively, for $E_+ = 5$ and 1 GeV, in the case of isoscalar target.

Fig. 9. The asymmetry A in units of 10^{-4} as a function of E_- for $\theta_+ = \theta_- = 15^\circ$, $\phi = 180^\circ$ and $E = 50$ GeV, in the Weingerg-Salam model with $\sin^2 \theta_W = 0.23$. The solid and dashed curves are for the isoscalar target at $E_+ = 5$ and 1 GeV, respectively.

Fig.10. The Bethe-Heitler differential cross section $d\sigma^{(+)} + d\sigma^{(-)}$ for $E_+ = 1$ GeV, $E_- = 10$ GeV and $E = 20$ GeV. The solid, dashed and dotted curves correspond to $\theta_+ = 5^\circ, 10^\circ$ and 15° , respectively, for the

isoscalar target.

- Fig.11. The asymmetry for the azimuthally symmetric lepton pair; $E_+ = E_-$, $\theta_+ = \theta_-$ and $\phi = 180^\circ$. The asymmetry is shown in units of 10^{-4} for the vector-like model of the charged lepton with $\sin^2\theta_W = 1/4$, while it vanishes for the Weinberg-Salam model. The solid, dashed and dotted curves correspond to $\theta_\pm = 5^\circ, 10^\circ$ and 15° , respectively, for the isoscalar target.
- Fig.12. The asymmetry A as a function of E_- for $\theta_- = 1^\circ$ and $E = 10$ GeV in the Weinberg-Salam model with $\sin^2\theta_W = 0.23$.
- Fig.13. The asymmetry A as a function of E_- for $\theta_- = 5^\circ$ and $E = 10$ GeV in the Weinberg-Salam model with $\sin^2\theta_W = 0.23$.
- Fig.14. The asymmetry A as a function of E_- for $\theta_- = 1^\circ$ and $E = 20$ GeV in the Weinberg-Salam model with $\sin^2\theta_W = 0.23$.
- Fig.15. The asymmetry A as a function of E_- for $\theta_- = 5^\circ, 10^\circ$ and $E = 20$ GeV in the Weinberg-Salam model with $\sin^2\theta_W = 0.23$. The solid and dashed curves correspond to $\theta_- = 5^\circ$ and 10° , respectively.
- Fig.16. The asymmetry A as a function of E_- for $\theta_- = 5^\circ, 10^\circ$ and $E = 50$ GeV in the Weinberg-Salam model with $\sin^2\theta_W = 0.23$. The solid and dashed curves correspond to $\theta_- = 5^\circ$ and 10° , respectively.
- Fig.17. The differential cross section, $d\sigma/dE_-d\Omega_- = (d\sigma^{(+)} + d\sigma^{(-)})/2dE_-d\Omega_-$, for the lepton pair production with unpolarized photons. It is shown as a function of the lepton energy E_- for the fixed angle at the incident photon energy of 20 GeV. The solid, dashed and dotted curves correspond to $\theta_- = 1^\circ, 5^\circ$ and 10° , respectively.

Table I. Summary of neutral currents comparison with the Weinberg-Salam model from ref. 3).

Process	Experimental results	$\sin^2 \theta$	W-S Prediction with $\sin^2 \theta = 0.23$
1. Purely leptonic			
$\bar{\nu}_e + e^- \rightarrow \bar{\nu}_e + e^-$	$(5.7 \pm 1.2) \times 10^{-42} E_\nu \text{ cm}^2$	0.29 ± 0.05	5.0
$\nu_\mu + e^- \rightarrow \nu_\mu + e^-$	$(1.7 \pm 0.5) \times 10^{-42} E_\nu \text{ cm}^2$	$0.21^{+0.09}_{-0.08}$	1.5
$\bar{\nu}_\mu + e^- \rightarrow \bar{\nu}_\mu + e^-$	$(1.8 \pm 0.9) \times 10^{-42} E_\nu \text{ cm}^2$	$0.30^{+0.10}_{-0.30}$	1.3
2. Elastic scattering			
$\nu_\mu + p \rightarrow \nu_\mu + p$	$(0.11 \pm 0.02) \times \sigma(\nu_\mu + n \rightarrow \mu^- + p)$	0.26 ± 0.06	0.12
$\bar{\nu}_\mu + p \rightarrow \bar{\nu}_\mu + p$	$(0.19 \pm 0.08) \times \sigma(\bar{\nu}_\mu + p \rightarrow \mu^+ + n)$	≤ 0.5	0.11
3. Single pion production			
$\nu_\mu + N \rightarrow \nu_\mu + N + \pi^0$	$(0.45 \pm 0.08) \times \sigma(\nu_\mu + N \rightarrow \mu^- + N + \pi^0)$	0.22 ± 0.09	0.42
$\bar{\nu}_\mu + N \rightarrow \bar{\nu}_\mu + N + \pi^0$	$(0.57 \pm 0.11) \times \sigma(\bar{\nu}_\mu + N \rightarrow \mu^+ + N + \pi^0)$	$0.15 - 0.52$	0.60
4. Inclusive			
$\nu_\mu + N \rightarrow \nu_\mu + \dots$	$(0.29 \pm 0.01) \times \sigma(\nu_\mu + N \rightarrow \mu^- + \dots)$	0.24 ± 0.02	0.30
$\bar{\nu}_\mu + N \rightarrow \bar{\nu}_\mu + \dots$	$(0.35 \pm 0.025) \times \sigma(\bar{\nu}_\mu + N \rightarrow \mu^+ + \dots)$	0.3 ± 0.1	0.38

Table II. Second-rank tensors constructed from P^μ and q^μ .

	Conserved	Nonconserved
Polar symmetric	$g_{\mu\nu} - \frac{q_\mu q_\nu}{q^2}$, $\left(P_\mu - \frac{P \cdot q}{q^2} q_\mu \right) \left(P_\nu - \frac{P \cdot q}{q^2} q_\nu \right)$	$q_\mu q_\nu, P_\mu q_\nu + P_\nu q_\mu$
Polar antisymmetric	...	$P_\mu q_\nu - P_\nu q_\mu$
Axial symmetric
Axial antisymmetric	$\epsilon_{\mu\nu\alpha\beta} P^\alpha q^\beta$...

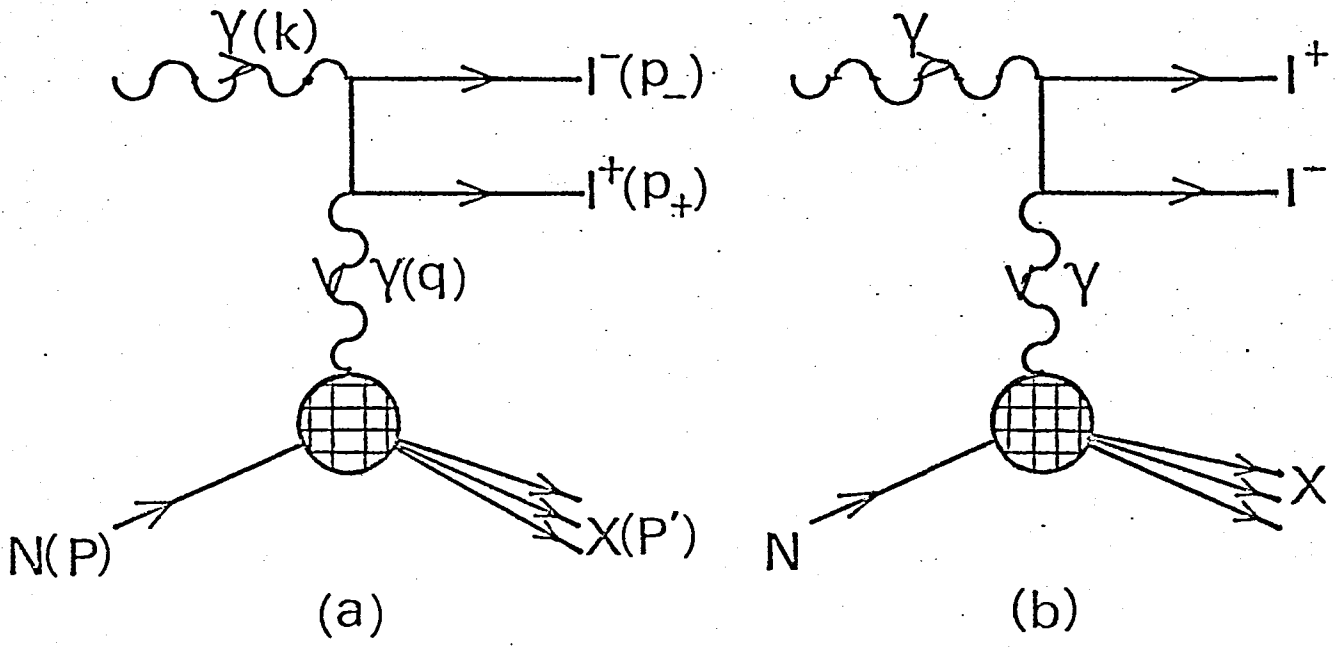


Fig.1

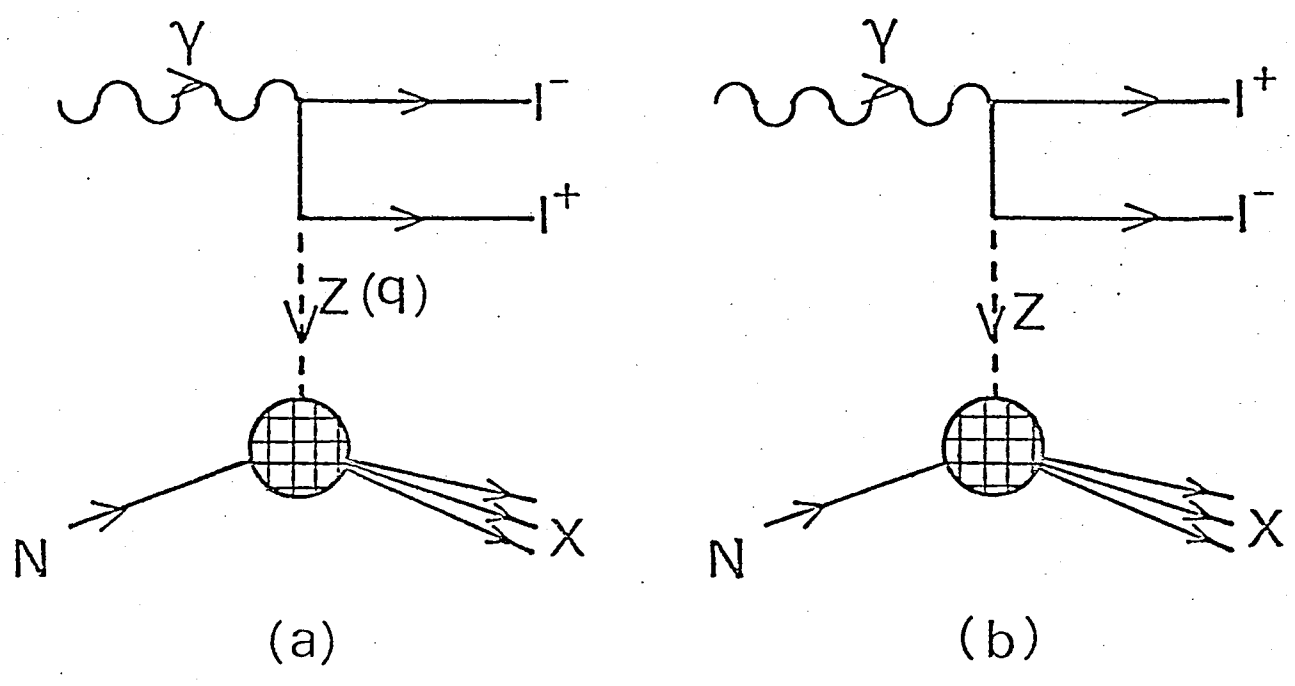
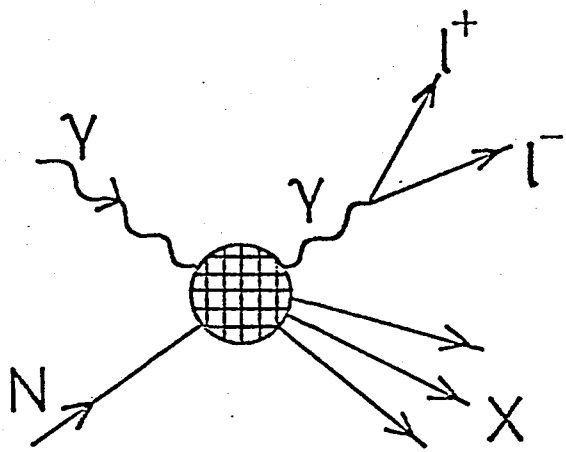
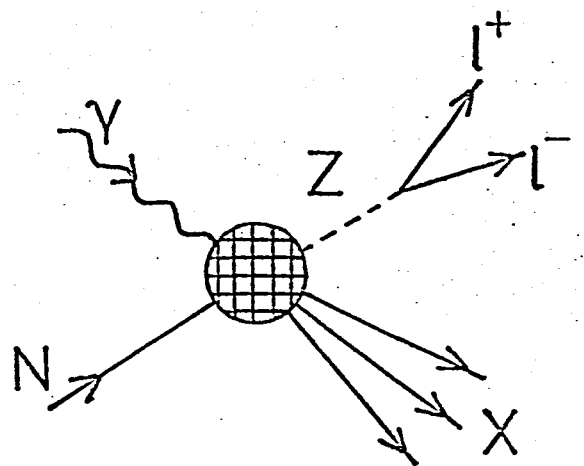


Fig. 2



(a)



(b)

Fig.3

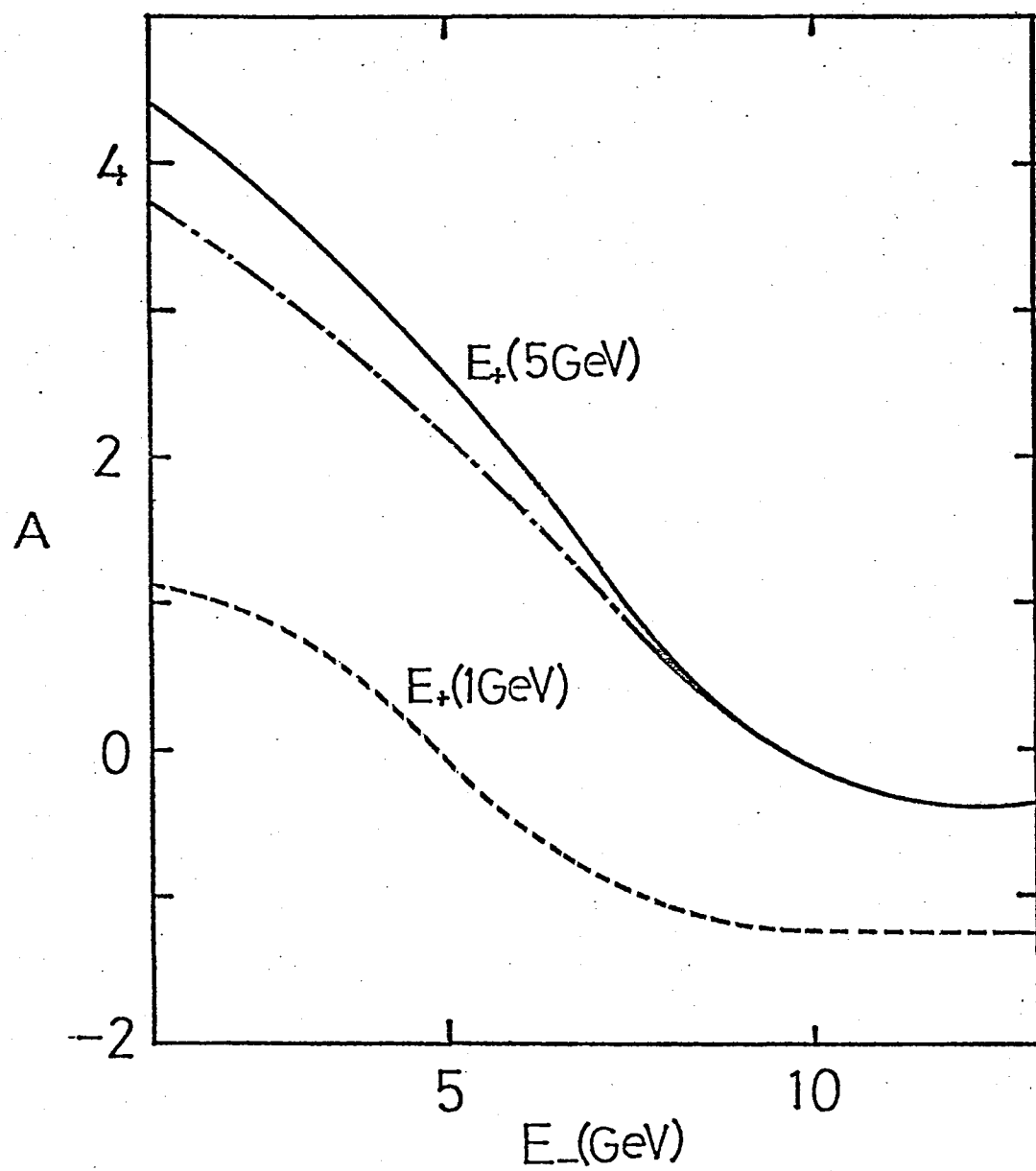


Fig.4

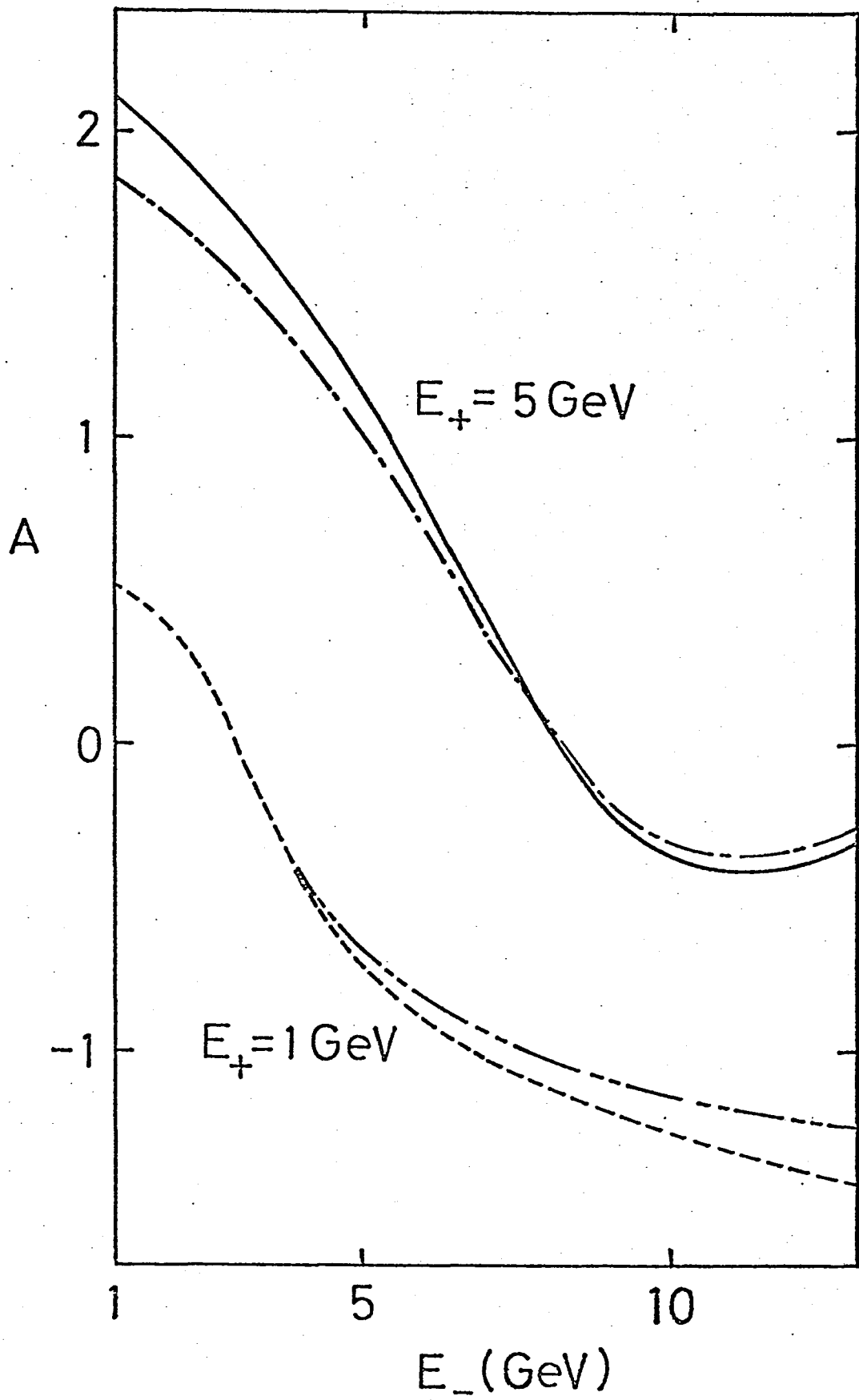


Fig.5

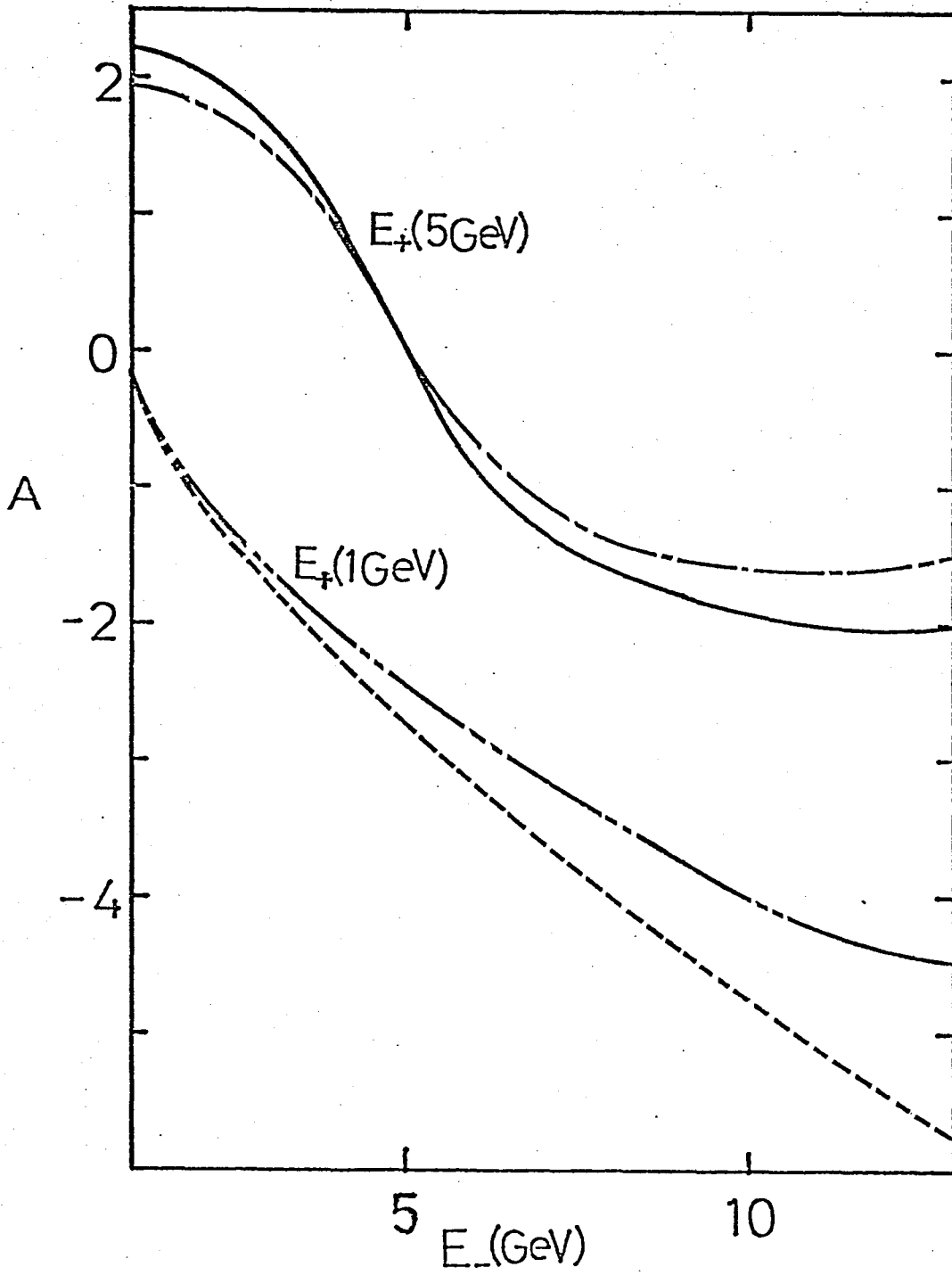


Fig. 6

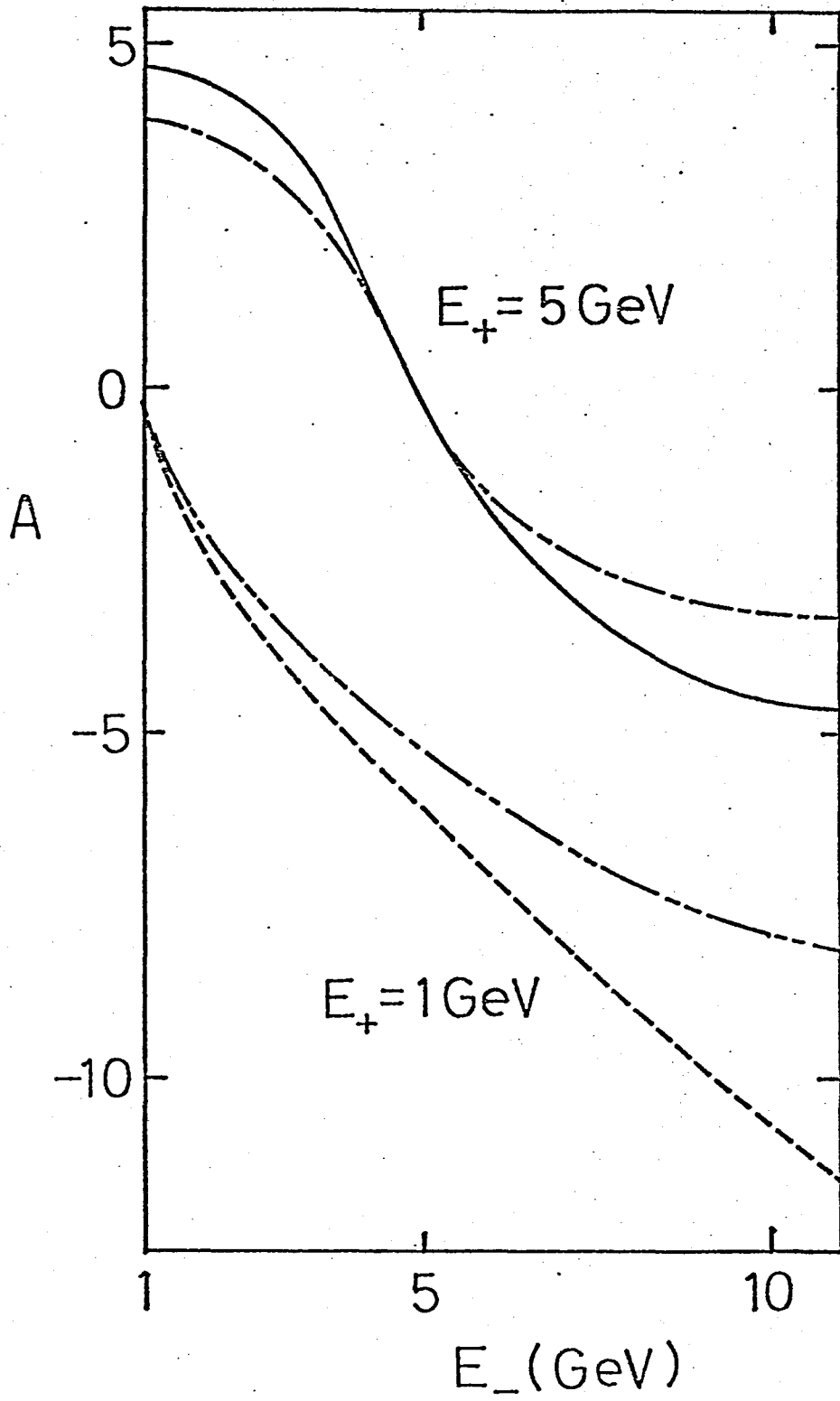


Fig.7

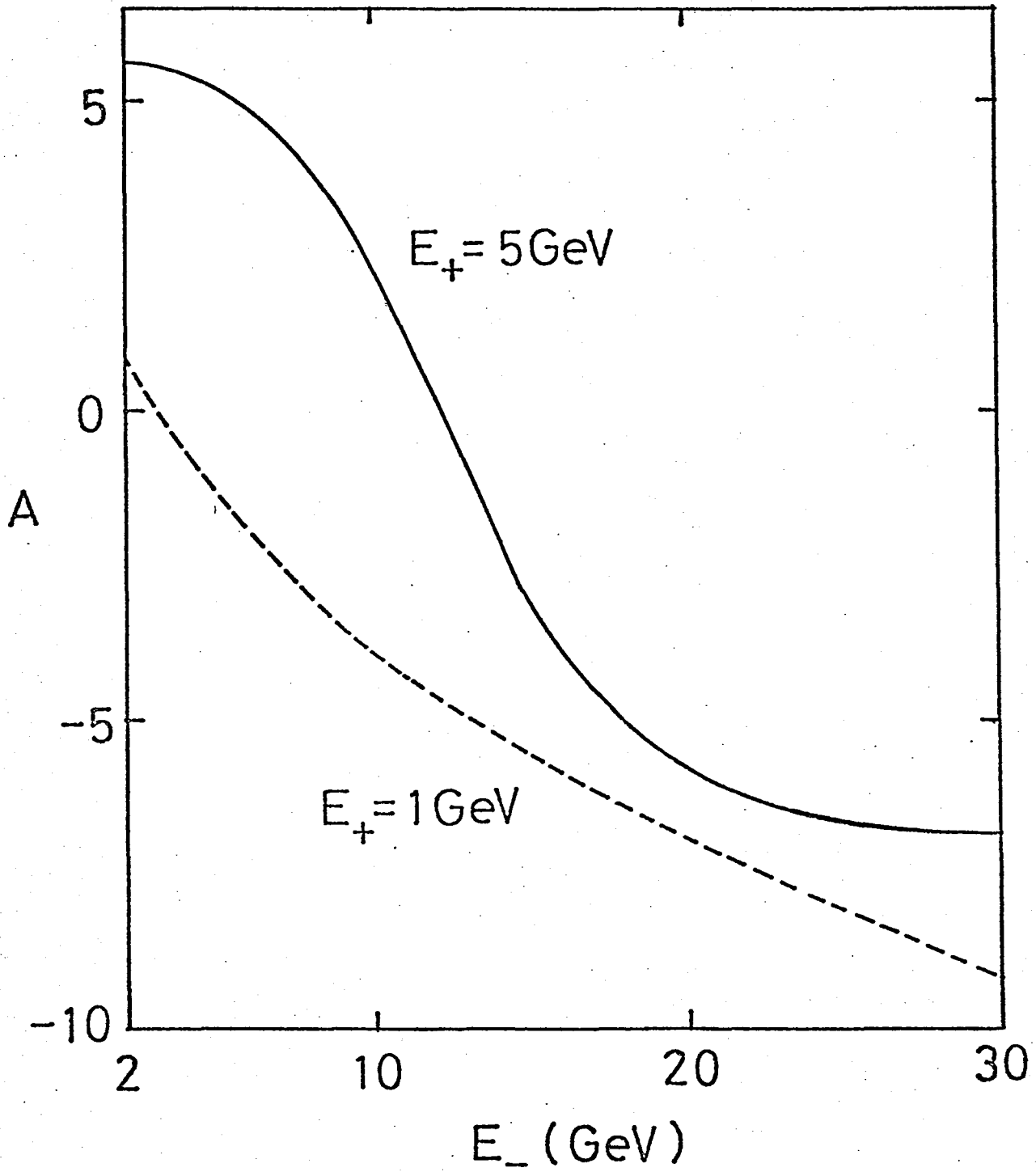


Fig.8

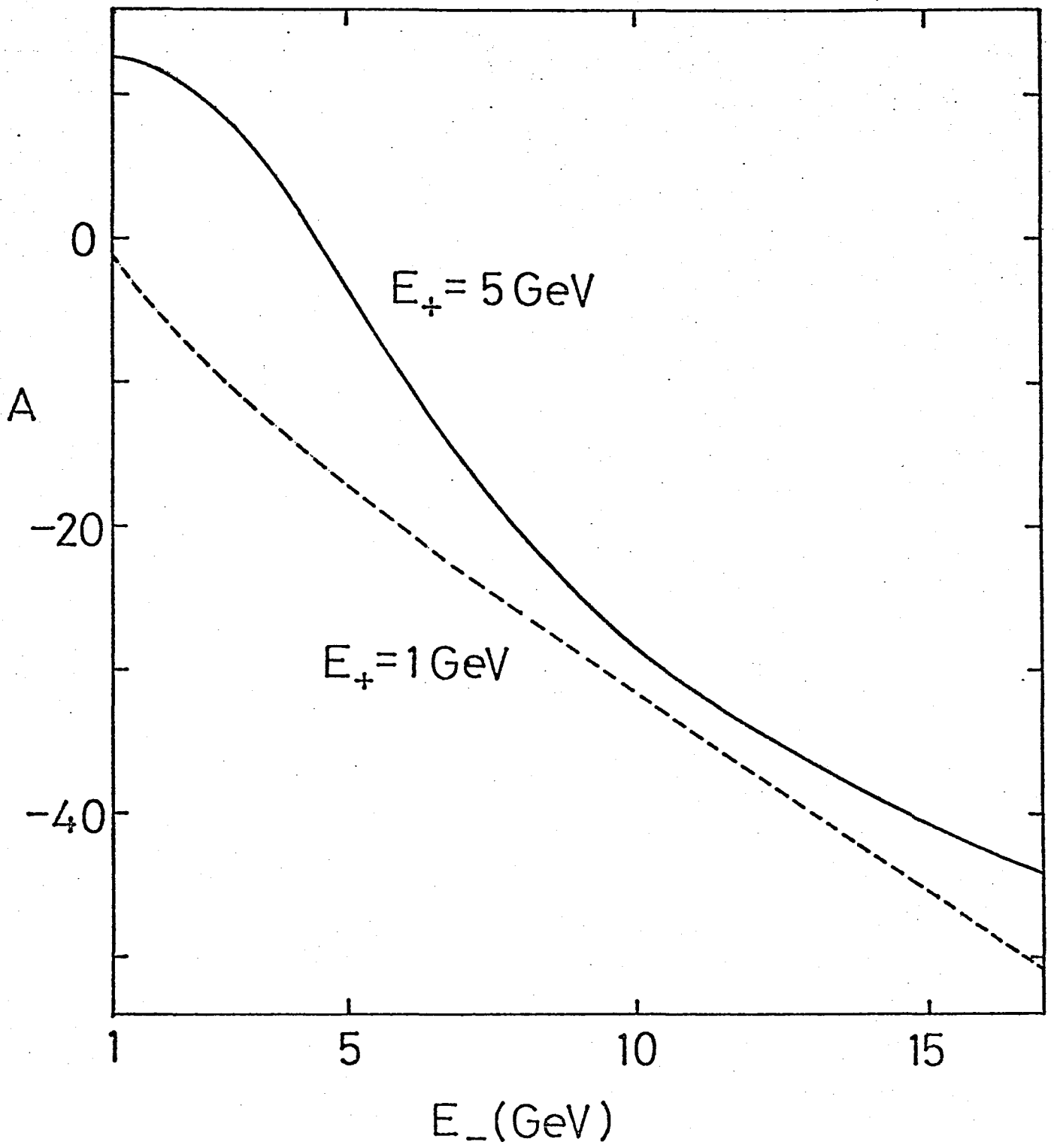


Fig.9

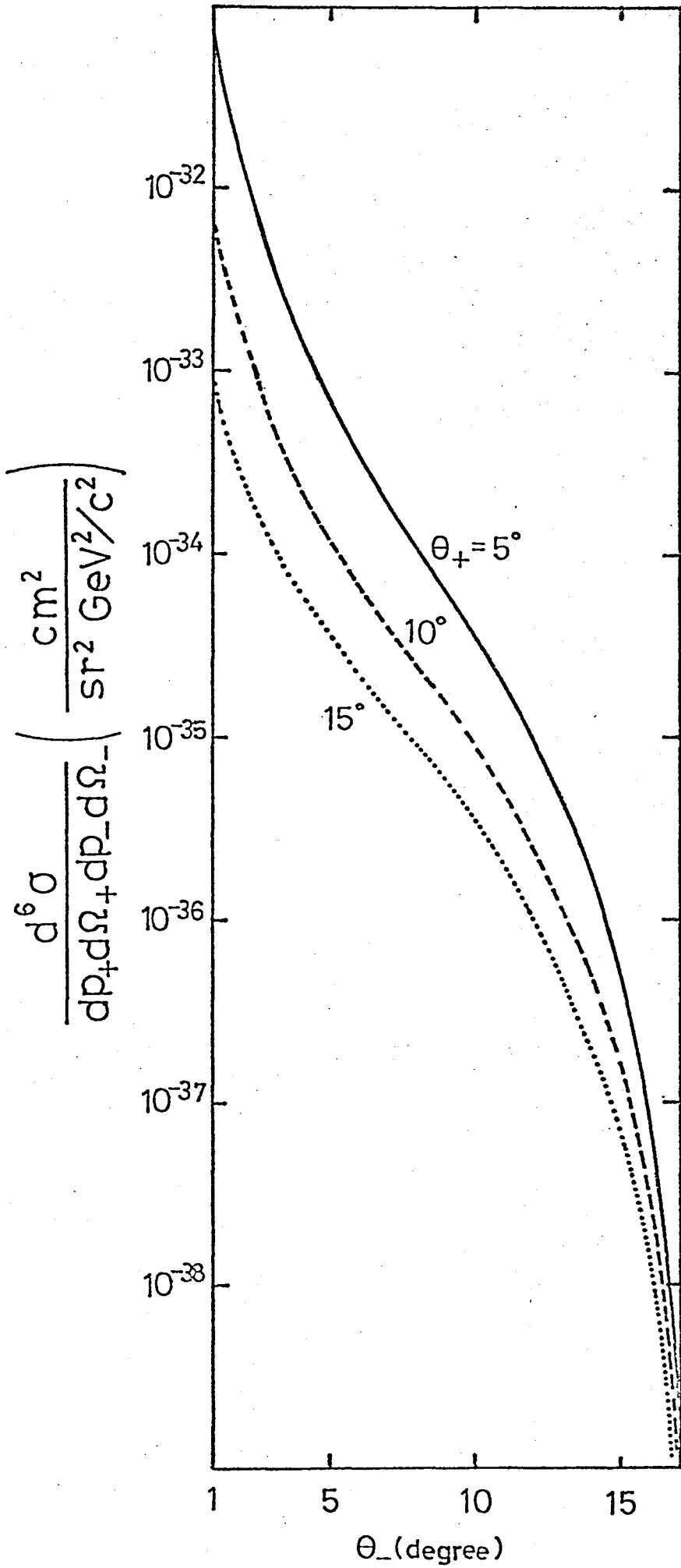


Fig.10

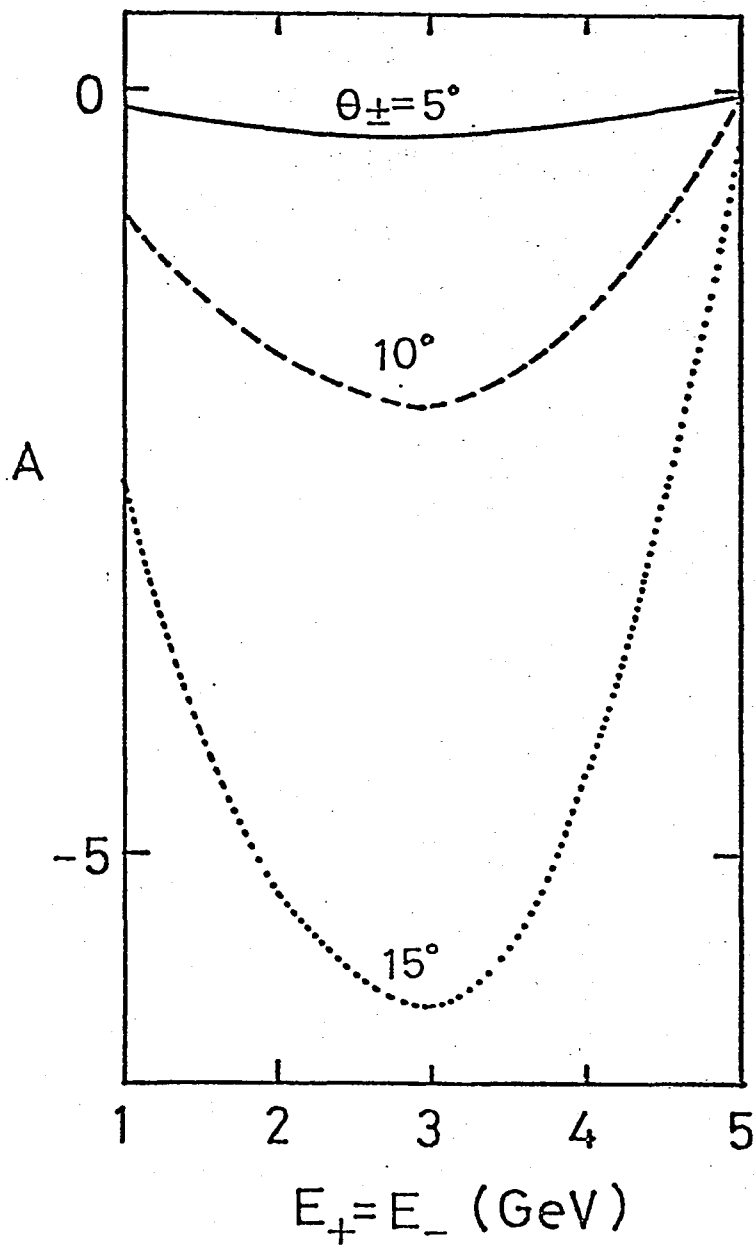


Fig.11

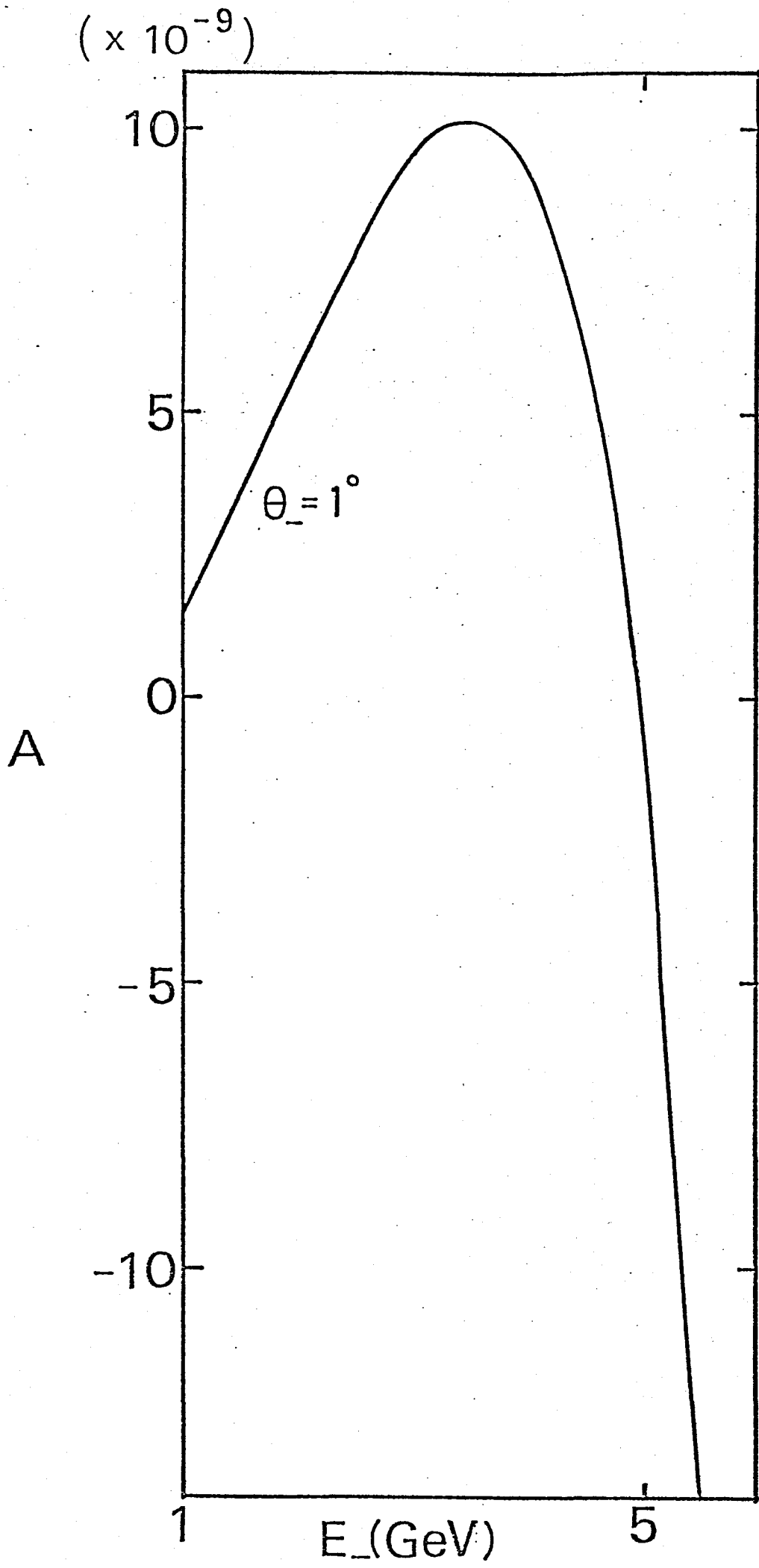


Fig.12

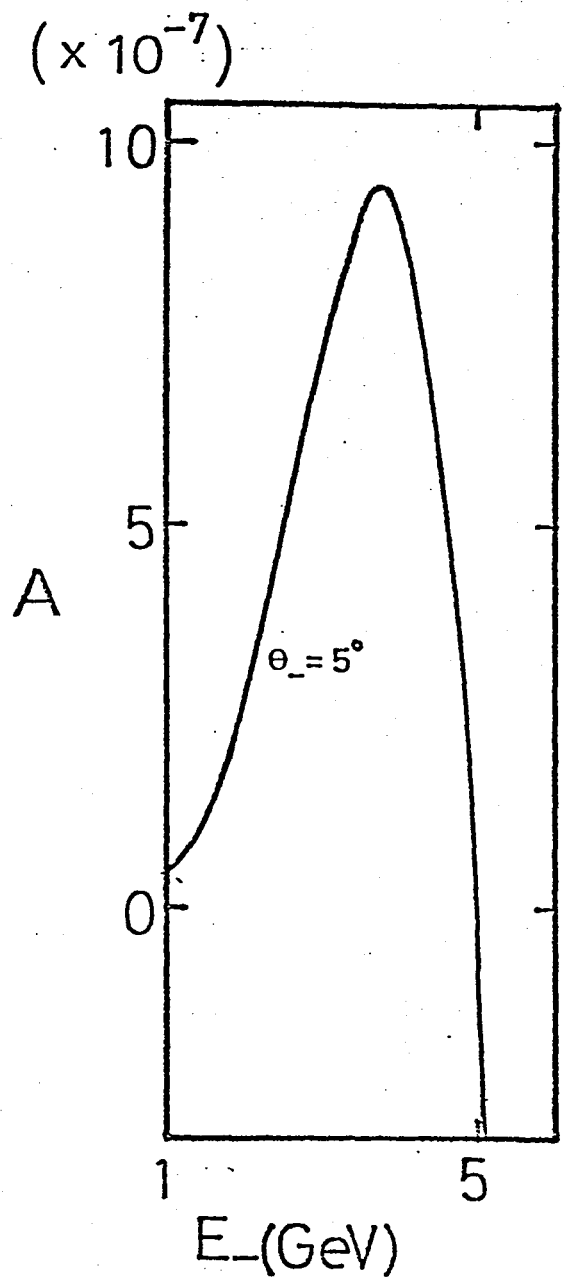


Fig.13

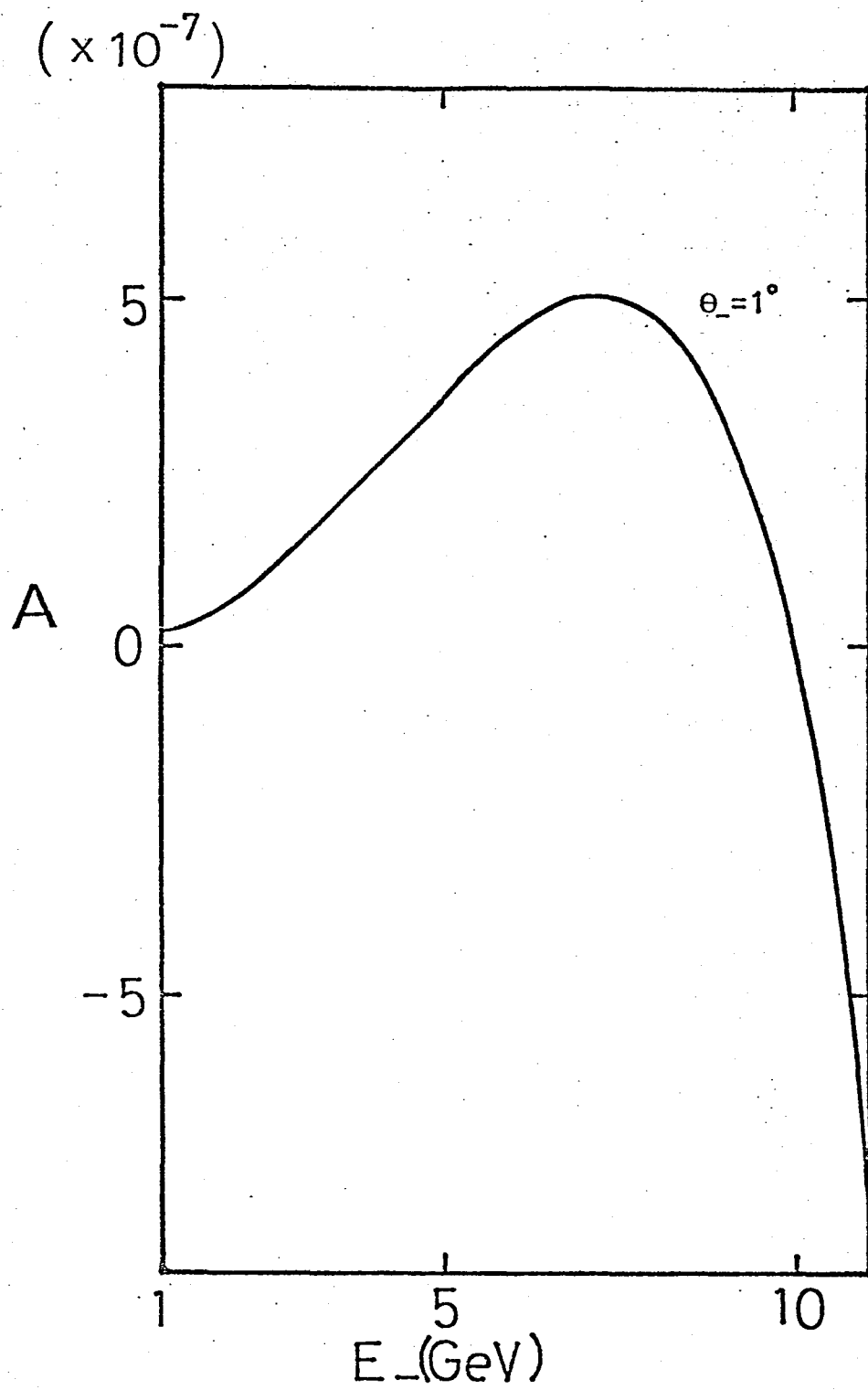


Fig.14

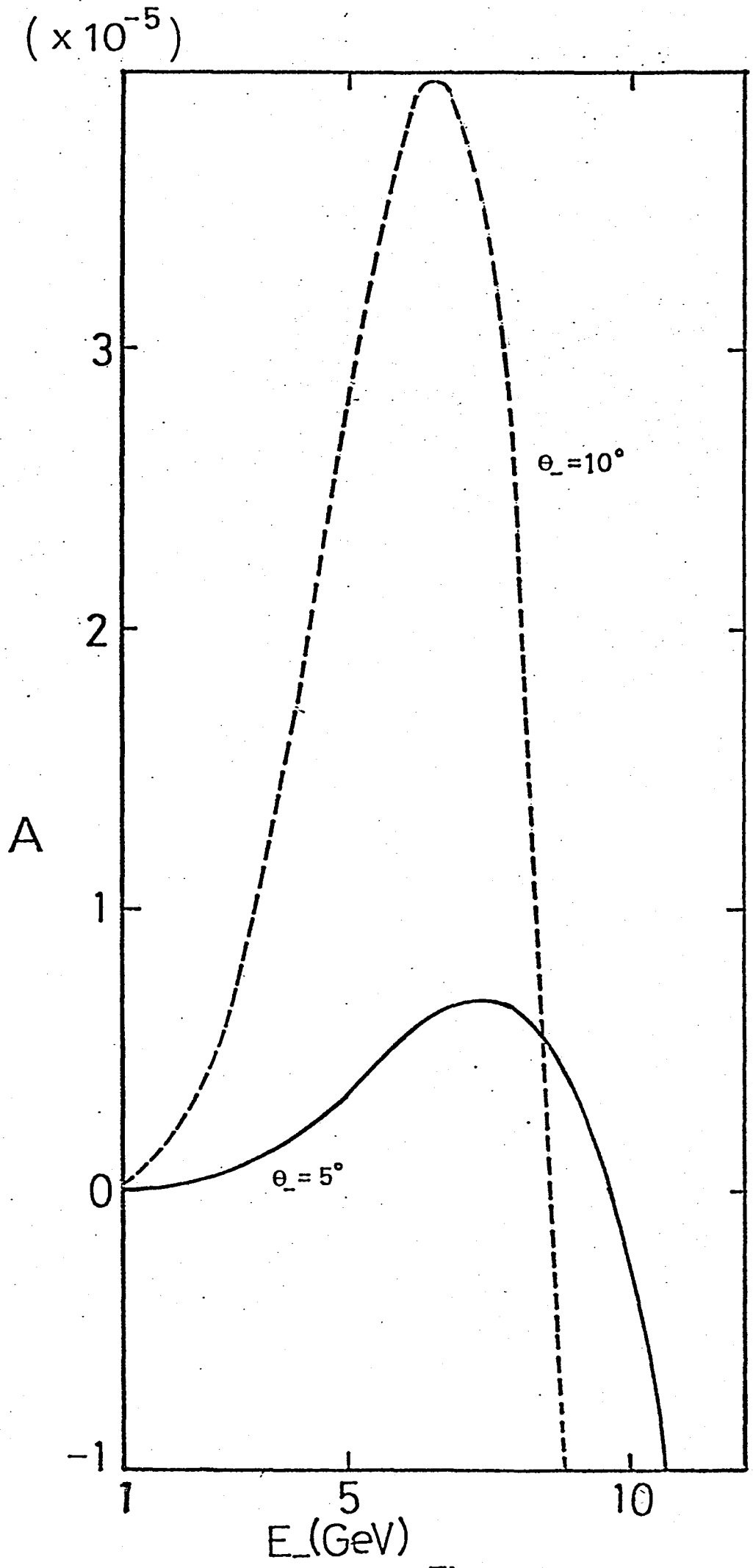


Fig.15

($\times 10^{-4}$)

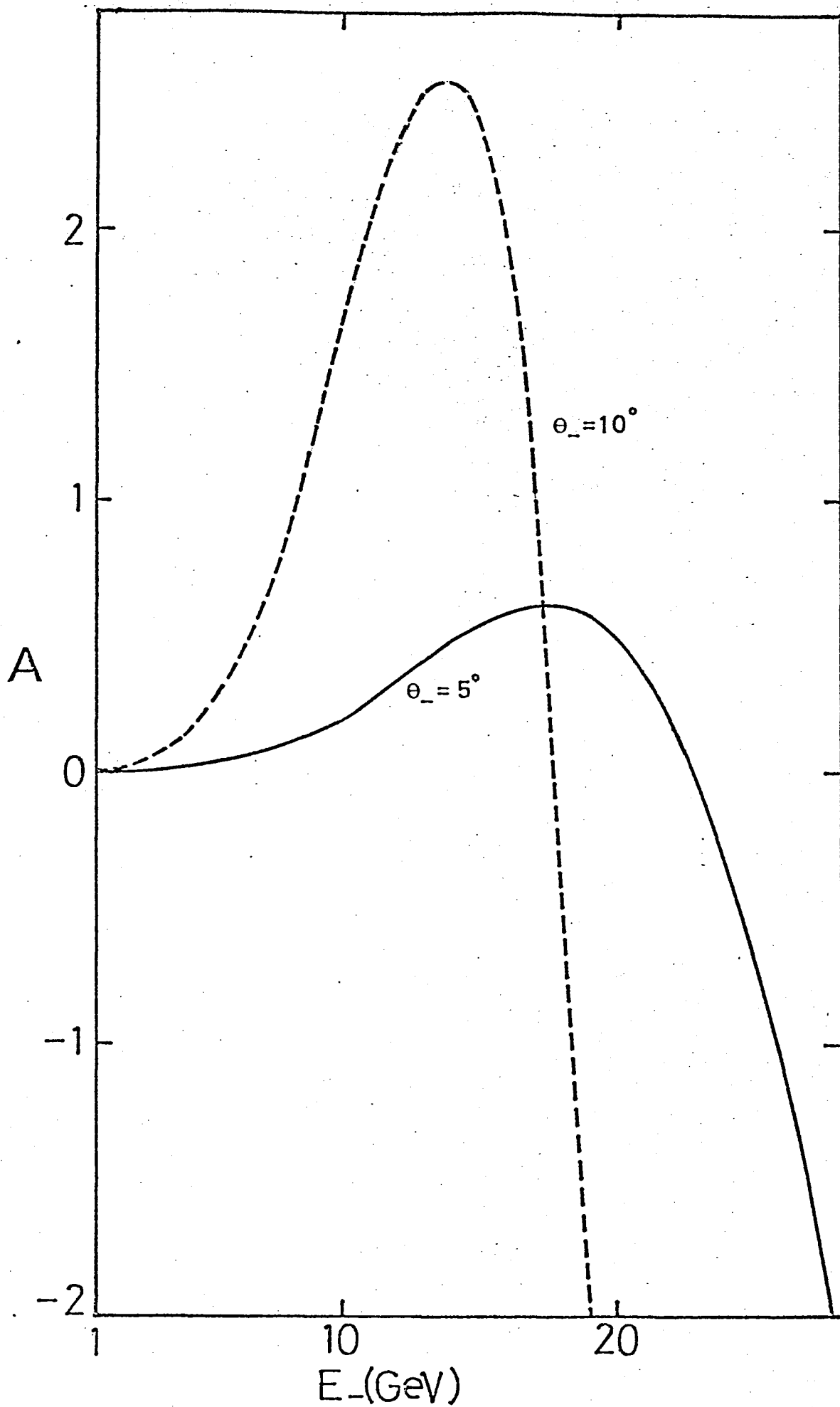


Fig.16

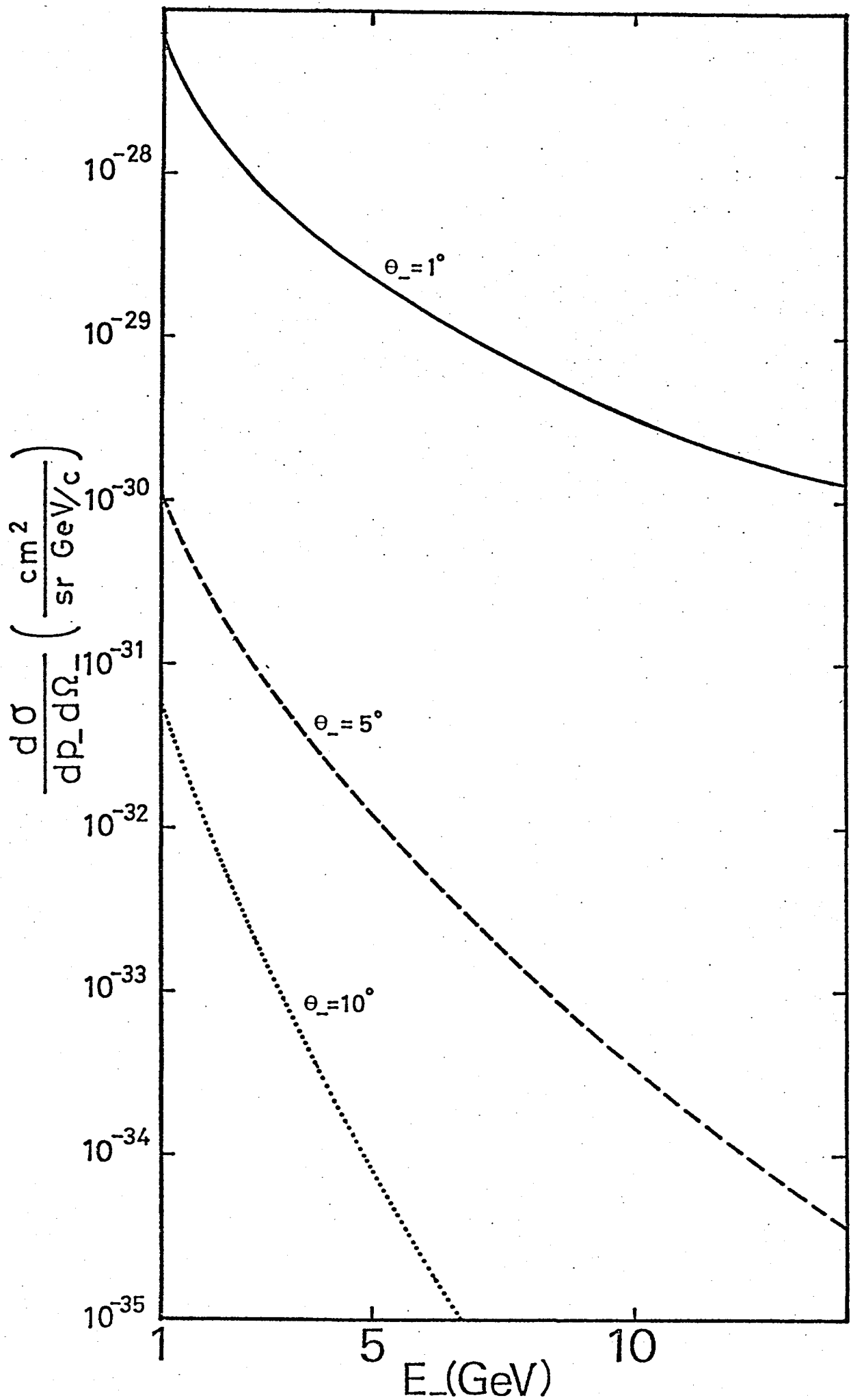


Fig.17